Z. Geomorph. N.F.	53	Suppl. 1	1 – 37	Berlin · Stuttgart	Juni 2009

The Lake Voulkaria (Akarnania, NW Greece) palaeoenvironmental archive – a sediment trap for multiple tsunami impact since the mid-Holocene

A. Vött, H. Brückner, S.M. May, D. Sakellariou, O. Nelle, F. Lang, V. Kapsimalis, S. Jahns, R. Herd, M. Handl and I. Fountoulis

with 14 figures 1 table

Summary. This paper presents evidence of multiple tsunami impact on the near-coast freshwater lake environment of the Lake Voulkaria (Akarnania, NW Greece) since the mid-Holocene. Detailed stratigraphies are given for 10 vibracores from the western and southwestern shores completed by additional geo-scientific information from all around the lake. Sedimentological, macro- and micropalaeontological, micromorphological, geochemical and geophysical methods were applied to differentiate between autochthonous quiescent water mud and intersecting layers of allochthonous material out of sand, gravel, marine shell and foraminiferal debris, organic matter and/or ceramic fragments. Arguments against interpreting high-energy sediments as storm or temporary sea level highstand deposits are discussed in detail.

Analysing the Lake Voulkaria sediment trap and the adjacent Bay of Cheladivaron revealed a sequence of four tsunami generations. Geochronostratigraphic interpretations are based on relative palynological age determination, radiocarbon dating and geoarchaeological findings. The oldest tsunami (generation I) did probably not affect the lake itself but connected the former Lake of Cheladivaron to the open Ionian Sea; this event took place in the 6th millennium BC or shortly afterwards. The subsequent tsunami generation II is dated to around 1000 cal BC; the following generation III hit the lake most probably during Classical-Hellenistic to maximum Roman times. Thick deposits of tsunami generation IV from the 4th century AD were encountered all around the lake, probably representing traces of the well-known 365 AD earthquake and tsunami catastrophe that destroyed large parts of the eastern coastal Mediterranean. We found generally good accordance in number and age between tsunami sediments found in the Lake Voulkaria and tsunami traces from adjacent coastal sites described in previous papers. This study revealed the Lake Voulkaria to be an outstanding tsunami sediment trap highly valuable to establish a local geochronology for extreme events in the northwestern Ionian Sea.

Zusammenfassung. In diesem Beitrag werden Belege für mehrfachen Tsunami-Einfluss auf den Voulkaria-See, einen küstennahen Süßwassersee in Akarnanien (Nordwestgriechenland), vorgestellt. Der detaillierte stratigraphische Aufbau von 10 Schlaghammerbohrprofilen des westlichen und südwestlichen Seeufers wird präsentiert und durch zusätzliche Informationen aus zahlreichen weiteren Bohrungen im gesamten Umfeld des Sees ergänzt. Sedimentologische, makro- und mikropaläontologische, mikromorphologische, geochemische und geophysikalische Methoden wurden angewandt, um zwischen autochthonen tonig-schluffigen Stillwasserablagerungen und zwischengeschalteten Schichten allochthonen Materials zu differenzieren. Letztere bestehen aus Sand, Kies, Grus, Gehäuse- und Schalenfragmenten mariner Mollusken und Foraminiferen, organischer Substanz und/oder Keramikfragmenten. Argumente gegen die Interpretation dieser Hochenergie-Ablagerungen als Sturmsedimente oder Sedimente eines zwischenzeitlichen Meeresspiegelhochstandes werden ausführlich diskutiert.

Die Untersuchung der Sedimentfallen des Voulkaria-Sees und der angrenzenden Bucht von Cheladivaron erbrachte eine Sequenz von vier unterschiedlichen Tsunami-Generationen. Geochronostratigraphische Interpretationen basieren auf relativer palynologischer Altersbestimmung, Radiokohlenstoffdatierungen und geoarchäologischen Befunden. Das älteste Tsunami-Ereignis (Generation I) führte zur Anbindung eines frühen Cheladivaron-Sees an das Ionische Meer und fand wahrscheinlich bereits im

DOI: 10.1127/0372-8854/2009/0053S1-0001 0372-8854/09/5301-0001 $ 9.25

6. Jahrtausend v. Chr. oder kurz darauf statt. Die nächstfolgende Tsunami-Generation II wird auf die Zeit um 1000 cal BC datiert. Das Ereignis der Generation III fand wahrscheinlich in klassisch-hellenistischer bis römischer Zeit statt. Mächtige Ablagerungen der Tsunami-Generation IV wurden im Umfeld des gesamten Sees gefunden und stammen aus dem 4. Jahrhundert n. Chr. Wahrscheinlich stellen sie Spuren der bekannten Erdbeben- und Tsunami-Katastrophe von 365 AD dar, die zur Zerstörung ausgedehnter Küstenabschnitte im östlichen Mediterranraum geführt hat. Anzahl und Alter der Tsunami-Ablagerungen aus dem Voulkaria-See stimmen im Allgemeinen gut mit Tsunami-Spuren an benachbarten Küstenabschnitten überein, die in früheren Studien erfasst wurden. Die vorliegende Untersuchung zeigt, dass der Voulkaria-See eine ausgezeichnete und höchst wertvolle Sedimentfalle für die Erstellung einer lokalen Chronologie für Extremereignisse im nordwestlichen Ionischen Meer darstellt.

1 *Introduction*

Scientific efforts to document, analyze and reconstruct palaeo-tsunami events in the Mediterranean Sea have been considerably intensified during the past decade. This is mostly due to the catastrophic 2004 Southeast Asia tsunami and the following rise of public and political interest in tsunami risk issues. One major lesson learned for the Mediterranean is that reaction times after a tsunamigenic earthquake will be very short due to the many interacting basins with their different morphologies, their highly complex coastline configurations and the locally very short shore-to-shore distances (see Pareschi et al. 2006). Major faults and subduction zones as well as steep bathymetrical conditions highly apt to produce submarine mass movements make the tsunami risk in the eastern Mediterranean to one of the largest all over the world with statistical re-occurrence rates of up to 8–11 years for extreme events regardless of their intensity (Soloviev et al. 2000, Schielein et al. 2007). Many geo-scientific and historical studies have revealed evidence of numerous tsunami events since the mid-Holocene. In contrast, in Southeast Asia, geo-science just started to look for past analogies of the 2004 event (Jankaew et al. 2008). However, the Mediterranean has been spared from larger destructive events for several centuries so that public risk awareness is quite weak.

Palaeo-tsunami studies in the eastern Mediterranean focused on different types of tsunami traces. A first group comprises dislocated slabs and blocks out of bedrock encountered along the coasts of southern Italy (Mastronuzzi & Sansò 2000, 2004, Mastronuzzi et al. 2007, Scicchitano et al. 2007), Greece (Scheffers & Scheffers 2007, Vött et al. 2006a, 2008a), Turkey (Kelletat 2005) and the Levante (Morhange et al. 2006) that are interpreted to be moved by tsunami force from their original positions. The second group includes ex-situ allochthonous sand and gravel deposits as well as shell debris layers detected in supra- or non-littoral positions (e.g. for Italy: Gianfreda et al. 2001; for Greece: Pirazzoli et al. 1999, Dominey-Howes et al. 2000, Gaki-Papanastassiou et al. 2001, McCoy & Heiken 2000, Kortekaas 2002, Vött et al. 2007a, 2008b; for Cyprus: Kelletat & Schellmann 2002; for Turkey: Minoura et al. 2000: for the Levante: Reinhardt et al. 2006) which are beyond the range of modern-day storms. The third type is cultural debris such as ceramic fragments and terrigenous material mixed up with high-energy marine deposits found in geoarchaeological contexts. In Crete, such mixed deposits could be attributed to a tsunami triggered by the Santorini eruption in the 17th century BC (Bruins et al. 2008). The fourth type are sequences of allochthonous high-energy

marine deposits intersecting near-shore lagoonal sediments; where storm influence can be excluded, these sequences represent interferences of quiescent sedimentary environments by multiple tsunami impact (e.g. for Greece: Kontopoulos & Avramidis 2003, Vött et al. 2007b, 2008c; for the western Mediterranean e.g. Becker-Heidmann et al. 2007).

In palaeo-tsunami studies, it is important to distinguish safely between storm and tsunami influence. From a sedimentological point of view, a set of characteristics was found to be typical of tsunami imprint (Dawson 1994, Dominey-Howes et al. 2006, Dawson & Stewart 2007, Kortekaas & Dawson 2007, Morton et al. 2007). One of the most difficult tasks, however, is to find appropriate sediment archives that allow establishing a comprehensive local to even regional tsunami chronology. With this respect, quiescent near-shore water bodies or swamps are the most promising candidates, especially concerning larger events that reached beyond the littoral zone where sedimentary traces are steadily endangered of erosion and reworking effects.

This paper focuses on the near-coast Lake Voulkaria freshwater environment in Akarnania, NW Greece (Fig. 1). Former studies revealed multiple tsunami impact on the adjacent Lefkada-Preveza coastal zone and showed that the lake was affected by a tsunami event around 1000 cal BC (Vött et al. 2006a, 2008d). The main objectives of this study were (i) to check for event stratigraphic traces of further tsunami deposits in the sediment trap, (ii) to document sedimentological, macro- and microfaunal, micromorphological and geochemical characteristics of allochthonous deposits, (iii) to establish a local tsunami chronology, (iv) to reconstruct tsunami flow patterns and clarify in which way settlements and human activities were affected in ancient times.

2 *Natural and archaeological settings and geotectonic background*

The Lake Voulkaria is located in northwestern Akarnania between the cities of Lefkada and Preveza (Fig. 1). It is separated from the inner Bay of Aghios Nikolaos (= Bay of Cheladivaron) by a N-S trending bedrock sill out of Triassic limestone and dolomite (IGME 1996) with elevations between maximum 18 m above sea level (m a.s.l.) in the north and minimum 5 m in the south (Fig. 2). The Bay of Aghios Nikolaos represents a former lagoonal environment that was originally closed off from the Ionian Sea by the ancient SSW-NNE running Plaka beachridge system some 5 km to the west of Aghios Nikolaos (Fig. 1). This former strandline was destroyed by multiple tsunami impact (Vött et al. 2006a, 2007a, 2008b). Its cemented beachrock base nowadays works as natural breakwater inducing moderate to even low-energy dynamics in the bay behind. Traces of severe tsunami landfall along the coast between Preveza and Lefkada comprise, for instance, fields of dislocated blocks and stones on top of the Cheladivaron Promontory, runup deposits in the inner Bay of Aghios Nikolaos, beachrock blocks and slabs dislocated towards the east of the Plaka, sharp erosional contacts of marine shell debris and sand layers on top of palaeosols (for further details see Vött et al. 2007a, 2008b, 2008c, 2008d, 2008e, May et al. 2007). In this context, a so called "Brown Layer" with marine fossils, fine sand, and abundant organic material that was encountered in core VOUL 1 from the profundal zone of the Lake Voulkaria was found to represent a tsunamigenic suspension deposit dating to 1000 cal BC (Jahns 2005, 2007, 2009, Vött et al. 2006a).

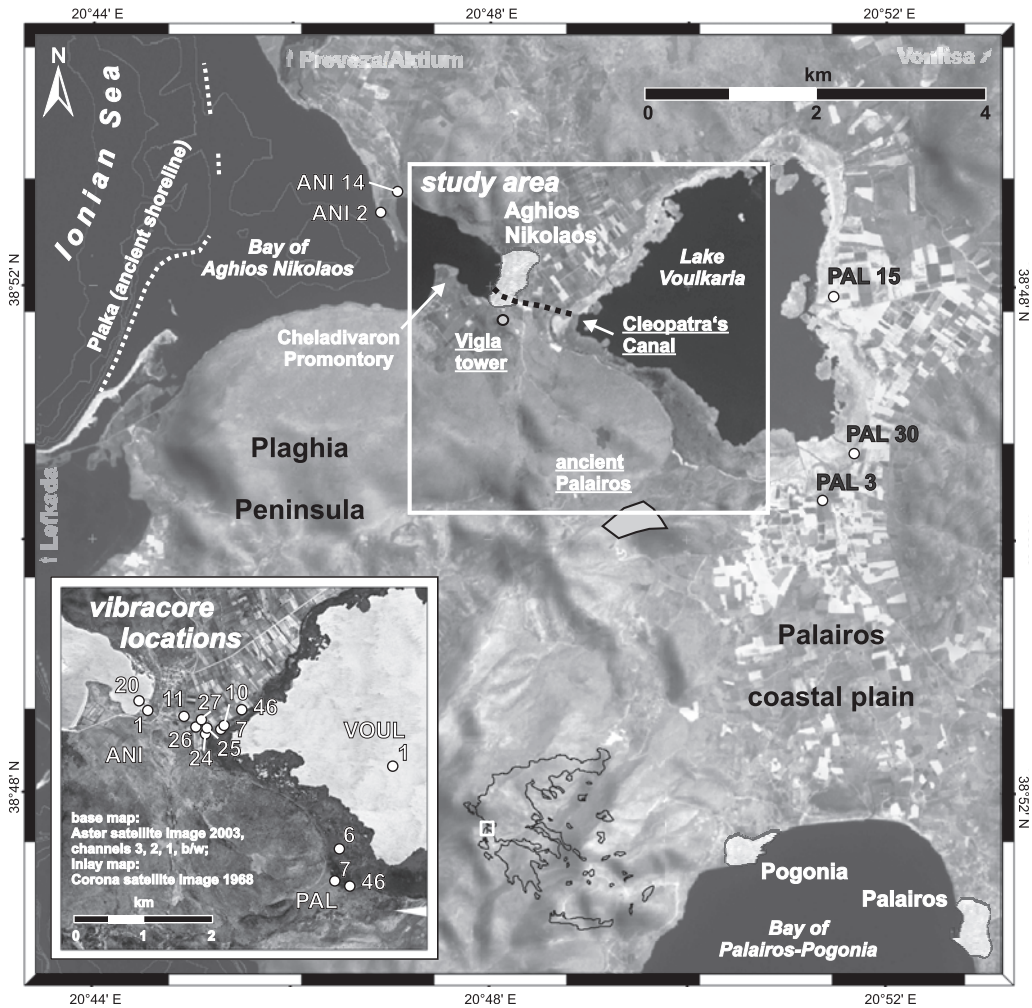

Fig. 1. Topographic overview of the Lake Voulkaria, the Bay of Aghios Nikolaos, and the Palairos coastal plain in northern Akarnania, NW Greece.

From a topographical point of view, special attention has to be paid for the overall funnel-like coastal configuration to the west of Aghios Nikolaos. The Bay of Cheladivaron has water depths mostly ≤ 1 m except from a narrow channel towards the modern harbour pier. The Phoukias sand spit separating the inner and outer bays of Aghios Nikolaos is younger than 1000 or so years most probably induced by a strong tsunami event (Vött et al. 2007a).

The Lake Voulkaria is situated in a polje-like depression on top of horizontally lying Triassic limestone in a graben situation (Bousquet 1976). Water depth is less than 3.5 m, the shores being accompanied by reed belts of *Phragmites* sp., up to 800 m wide. Recent studies showed that the

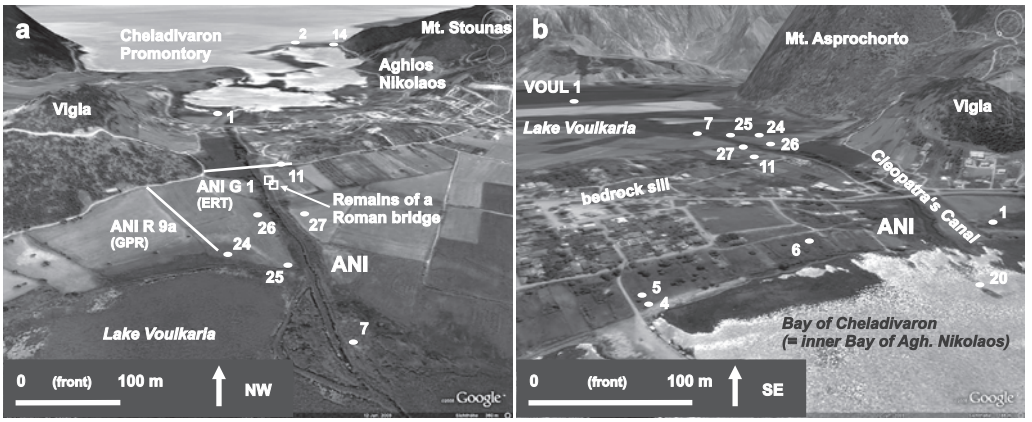

Fig. 2. Bird's eye views of the Aghios Nikolaos bedrock sill between the Lake Voulkaria and the inner Bay of Aghios Nikolaos. Digital elevation model and satellite image from GoogleEarth, vertical exaggeration 3x. View direction towards the NW (a) and the SE (b).

Lake Voulkaria is not the remnant of a former marine embayment extending inland across the modern Palairos coastal plain (Vött et al. 2006b, 2007b, see Fig. 1) but represents a freshwater lake environment existing at least since the 9th millennium BC (Jahns 2005).

The ancient city of Palairos is located on top of Kechropoula hill (266 m a.s.l.) to the southwest of the Lake Voulkaria, founded in the 6th century BC and first mentioned in 431 BC when the harbour of the neighbour town Sollion was handed over to the Palairotians by their Athenian allies (Lang et al. 2007). Between 330–326 BC, the poleis of Palairos and Lefkada imported cereals from Kyrene (northern Africa, Wacker 1996), which is possibly related to a strong tsunami event that hit the area around that time (Vött et al. 2008c). After the defeat of the Akarnanians in the Battle of Actium 31 BC, the city declined; however, the site remained occupied until Byzantine times (Lang et al. 2007). Cleopatra's Canal to the north of ancient Palairos was probably established (i) as an outlet during times of high water level especially during winter season and (ii) as a navigable waterway to a presumed lake harbour between the 5th and 1st cent. BC (Berkthold & Faisst 1993, see also Vött et al. 2006a, 2007b). An ancient tower on top of the nearby Vigla hill was part of an acropole in Classical-Hellenistic times and may have also been used as watch and signal tower before it was destroyed by an earthquake (Faisst & Kolonas 1990, Lang et al. 2007). The village of Aghios Nikolaos was founded in the 1920s by Greek refugees from Minor Asia.

The Plaghia Peninsula together with the Ionian Islands belongs to the seismically most active regions in the eastern Mediterranean (Papazachos & Papazachou 1997). Seismotectonic activity is related to the right-lateral strike slip Cefalonia transform fault (CF) and its northern prolongation, the Lefkada transform fault (LF), trending in a SSW-NNE direction offshore some 25 km to the west of Aghios Nikolaos (Karakostas et al. 2004). Here, collision, subduction, transform faulting, and spreading of the African, the Adriatic and the Aegean plates take place (Sachpazi et al. 2000, Hollenstein et al. 2008). Additionally, van Hinsbergen et al. (2005) and

Broadley et al. (2004) describe an average 40-90° clockwise rotation of northwestern Greece since Oligocene-Miocene times. High seismotectonic activity goes hand in hand with high tsunami risk (Papazachos & Dimitriu 1991). For the last strong earthquake on August 14, 2003 (Papadopoulos et al. 2003, Papadimitriou et al. 2006), a 0.5 m tsunami was reported from south of Nidri near Lefkada (EERI 2003). Historical accounts on tsunamis since ancient times have not yet been found, most probably due to the peripheral significance of this part of Greece; however, local tsunami catalogues based on historic and seismological data do exist (e.g. Vött et al. 2006a).

3 *Methods*

In this paper, we present detailed stratigraphic information of 10 vibracores drilled at the western and southwestern shores of the Lake Voulkaria by means of an engine driven Atlas Copco coring device (type mk 1). Maximum coring depth was 12 m below surface (m b.s.) using core diameters of 6 and 5 cm. Vibracores were photographed, described and sampled in the field, only core PAL 6 was taken as an inliner core and opened in the laboratory. On-site description comprised geomorphological, sedimentological and palaeontological criteria such as grain size distribution, grade of sorting, sediment colour, and determination of both species and state of preservation of macrofossil remains. We applied earth resistivity tomography by means of a multi-electrode Syscal R1 plus instrument and the RES2DINV inversion model as well as georadar studies using a RAMAC RTA instrument and an unshielded 50 MHz antenna to study subsurface structures and for spatial interpolation of vibracore data. A differential GPS system (type Leica SR 530) was used to determine the position and elevation of each coring site. In the laboratory, selected samples were analyzed for ostracods and foraminifers in order to detect allochthonous influence on the palaeoenvironmental record (Murray 2006). We used thin sections to check for sedimentary structures and fossil assemblages atypical of the quiescent freshwater lake conditions of the Lake Voulkaria. Standard geochemical parameters such as electrical conductivity, pH-value, loss on ignition, and concentrations of (ortho-)phosphate, calcium carbonate, (earth) alkaline and heavy metals were determined from a selection of sediment samples. Former studies showed that these parameters can be helpful in distinguishing sedimentary facies (Vött et al. 2002) and as geochemical fingerprints of tsunami impact (Vött et al. 2008c).

A geochronological frame was established using ^{14}C-AMS datings of organic samples or biochemically produced calcium carbonate. As dating of samples out of tsunamigenically reworked material yield sheer maximum ages and may result in age inversions in the geochronostratigraphy, we preferred taking samples out of undisturbed pre- or post-tsunami core sections where possible. The calibration software Calib 5.0.2. was used to calculate calendar ages. We corrected marine samples for an average reservoir effect of 402 years (Reimer & McCormac 2002) although the marine palaeo-reservoir effect might not have been constant through time and probably was subject to local variations (see Geyh 2005). Diagnostic ceramic fragments were rare in the cores; where found, we used them together with archaeological structures to cross-check radiocarbon ages. Palynological studies were helpful for relative dating based on comparisons with the detailed Lake Voulkaria pollen profile published by Jahns (2005, 2007, 2009).

4 *Event stratigraphy in the environs of the Aghios Nikolaos bedrock sill*

Information on event stratigraphy along transect A across the Aghios Nikolaos bedrock sill is presented for seven vibracores ANI 1, 11, 27, 26, 24, 25 and 7 running in a WNW-ESE direction (Figs. 1 to 3). We laid stress on sedimentary findings that clearly differ from modern environmental conditions in the Bay of Cheladivaron and the Lake Voulkaria which are characterized by quiescent waters with predominant deposition of silty to clayey shallow marine to lagoonal or freshwater sediments, respectively.

4.1 *Sedimentary record along vibracore transect A*

Vibracore ANI 1 (0.06 m a.s.l., N 38°51'56.4'', E 20°48'01.1'') was drilled on the southeastern shore of the Bay of Cheladivaron. The base of the profile shows light brown loamy deposits (11.94–11.21 m below sea level (= b.s.l.)), void of carbonate, representing weathered Pleistocene bedrock material (Figs. 1 to 3). This terrestrial unit is overlain by homogenous grey limnic mud (11.21–8.07 m b.s.l.) which, in its upper part, shows some intercalating peat layers. Pollen analysis of sample ANI 1/25 (10.18–10.06 m b.s.l.) revealed abundant pollen of *Myriophyllum spicatum* and *Nymphaea* sp. indicating pure freshwater conditions. On top of a following erosional unconformity, we found a layer of unsorted sand and marine shell debris (8.07–7.44 m b.s.l.) documenting an abrupt and sudden change towards saltwater conditions. Subsequently following lagoonal clay and silt including shells of *Cerastoderma glaucum* indicate that quiescent conditions were re-established (7.44–2.56 m b.s.l.). However, the lagoonal environment was influenced twice again by high-energy input of marine sand (6.94–6.09 m and 4.80–3.42 m b.s.l.). Finally, the lagoonal mud is covered by a thick layer of unsorted gravel, mostly consisting of chert and limestone fragments, and sand including abundant shell debris of marine organisms (2.56–0.69 m b.s.l.). The top of the profile is made out of clayey to silty marsh deposits.

Vibracoring site ANI 11 (4.50 m a.s.l., N 38°51'54.2'', E 20°48'15.2'') is located at the southeastern foot of the Aghios Nikolaos bedrock sill (Figs. 1 to 3). The profile shows thick clayey to silty limnic deposits (7.50–3.26 m b.s.l.) intersected by a layer of allochthonous fine sand (6.13–5.74 m b.s.l.). Another stratum of fine sand found at 3.26–2.18 m b.s.l. includes marine indicators. This layer was later covered by silty to clayey sediments of a lake which seems to have been affected by the secondary input of reworked coarse-grained material (fine sand and stones) by aeolian and colluvial processes (2.18–0.42 m b.s.l.). The upper part of the limnic unit consists of strongly weathered brown sediment (1.19–0.42 m b.s.l.) documenting the development of a palaeosol. The palaeosol is abruptly overlain by a thick layer of mostly unsorted beige sand, void of carbonate (0.42 m b.s.l. – 0.73 m a.s.l.), that itself is covered by weathered sand and gravel (0.73–2.55 m a.s.l.) with numerous chert fragments documenting another palaeosol unit. Subsequently follow autochthonous silty to clayey limnic sediments (2.55–3.28 m a.s.l.) accumulated in a local depression which was finally filled up by loamy to gravelly anthropogenic deposits.

Vibracore ANI 26 (5.15 m a.s.l., N 38°51'49.5'', E 20°48'28.5'') was drilled south of Cleopatra's Canal (Figs. 1 to 3). Its base is made up of silty to clayey limnic deposits (6.85–6.37 m b.s.l.). Marked by an erosional contact, limnic deposits are abruptly covered by a very thick layer of predominantly sandy sediments (6.37–3.27 m b.s.l.) that are fairly unsorted and include pebbles, grus, abundant

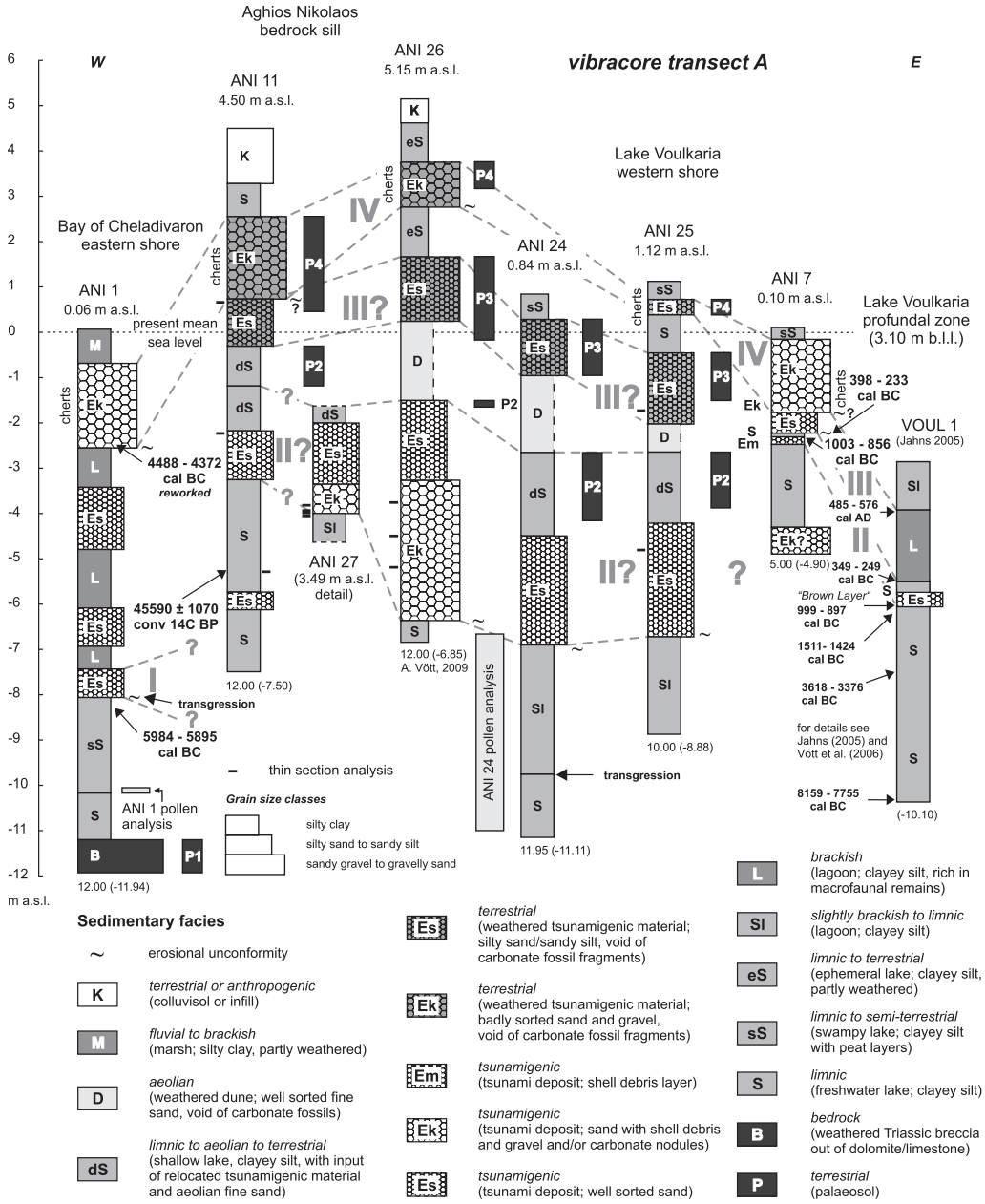

Fig. 3. Stratigraphies and vertical facies distribution for vibracores of transect A across the Aghios Nikolaos bedrock sill (for location of transect see Figs. 1 and 2, and Fig. 12 for photos of selected vibracore sections).

fragments of a marine macrofauna (e.g. *Ostrea* sp., *Loripes lacteus*, *Cerithium vulgatum*) and many carbonate nodules. Then, a stratum of well sorted fine to mean sand (3.27–1.50 m b.s.l.) follows; it is void of carbonate and shows, in its upper part, a thin palaeosol. Due to its laminated structure and the very good grade of sorting, the subsequent decalcified fine sand (1.50 m b.s.l. – 0.24 m a.s.l.) is interpreted as aeolian deposit reflecting intense reworking of ex-situ littoral sediments. The following unit of fine (and in comparable stratigraphic positions of cores ANI 24 and 25 also mean) sand is strongly weathered to a sandy to loamy palaeosol (0.24–1.66 m a.s.l.). This ex-situ sand is overlain by autochthonous limnic mud (1.66–2.76 m a.s.l.). The mud itself is covered by another section of decalcified sand and gravel (2.76–3.75 m a.s.l.) which contains a lot of chert fragments, up to 2 cm in diameter, representing another high-energy impact on the site. Finally, limnic conditions were re-established (3.75–4.62 m a.s.l.) and, subsequently, colluvial sediments were deposited (4.62–5.15 m a.s.l.).

Vibracores ANI 27 (2.49 m a.s.l., N 38°51'52.4'', E 20°48'31.1''), ANI 24 (0.84 m a.s.l., N 38°51'46.7'', E 20°48'33.1''), and ANI 25 (1.12 m a.s.l., N 38°51'49.3'', E 20°48'35.5'') differ from the ANI 26 stratigraphy only in some details. First, the bases of cores ANI 24 and 27 show a clear change from limnic to slightly brackish conditions similar to the one found for core ANI 1. Second, coarser-grained deposits of mid-core sections of cores ANI 24, 25 and 27 are covered by sediments of a limnic environment into which event-borne material was secondarily accumulated and then weathered to form palaeosols. Third, the uppermost layer of allochthonous material including indicative chert fragments was found in cores ANI 26 and 25 but not in core ANI 24. This may reflect event-related erosion around ANI 24 while adjacent sites were primarily subject to sediment deposition.

Vibracore ANI 7 (0.10 m a.s.l., N 38°51'48.2'', E 20°48'42.8'') marks the eastern end of transect A drilled some 15 m to the north of Cleopatra's Canal (Figs. 1 to 3). At its base, we found numerous limestone fragments embedded in a clayey to silty matrix (4.90–4.31 m b.s.l.); additional findings of sand may account for high-energy impact from the seaside. Subsequently, homogenous limnic mud (4.31–2.23 m b.s.l.) was encountered. In its upper part, it is intersected by a shell debris layer consisting of freshwater species and rich in organic matter indicating a temporary collapse of the environment. On top of an erosional unconformity, the limnic unit is abruptly covered by sand (2.23–1.77 m b.s.l.) including shell fragments of *Tellina* sp., *Cyclope neritea* and other marine species. Then, another erosional contact marks the change towards a gravel layer (1.77–0.16 m b.s.l.) with marine shell debris, ripup-clasts out of limnic mud and abundant chert fragments, up to 3 cm large. This event layer is finally overlain by autochthonous silty organic-rich deposits of a swampy lake.

In a summary view (Fig. 3), vibracore transect A across the Aghios Nikolaos bedrock sill shows that (i) the autochthonous sedimentary environments in the Bay of Cheladivaron and around the Lake Voulkaria, characterized by homogenously silty to clayey, partly swampy deposits, were repeatedly influenced by high-energy impact from the marine side as evidenced by repeatedly intersecting layers of sand and gravel and marine shell debris. These intersecting layers are interpreted as traces of tsunami landfalls; (ii) the onset of saltwater conditions in the Bay of Cheladivaron is bound to the sudden and abrupt cessation of the originally limnic environment by high-energy input of marine deposits; (iii) input of allochthonous material was fol-

lowed by subaerial weathering including decalcification and soil formation where the material was deposited above the sea level at that time – comprising the destruction of marine shell fragments. In contrast, marine biogenic carbonate was preserved in case of deposition under water; (iv) man-made indicators such as ceramic fragments, building material or stratigraphic disturbances were not found in cores of transect A. Hence, large-scale anthropogenic impact can be excluded as source of allochthonous deposits. This is also true because of the large thickness and the widespread distribution of ex-situ coarse-grained deposits along the shores of the Lake Voulkaria (see also Section 6, Fig. 12); (v) torrential activities can also be excluded as potential source because there are no alluvial fan systems existing all around the Aghios Nikolaos bedrock sill.

4.2 *Micro- and macrofossil and thin section analyses of event layers*

Microfossil analyses were carried out for samples from the allochthonous high-energy sand encountered in core ANI 25 between 6.73–4.22 m b.s.l. on top of an erosional unconformity. Fig. 4 shows the position of the samples with regard to the vertical facies distribution. The fairly unsorted base of the unit (samples 4 and 3) reflects the abrupt occurrence of 45 different species of fully marine origin. From the encountered faunal assemblage, only the bivalves *Cerastoderma glaucum*, *Lentidium mediterraneum*, the foraminifer *Ammonia beccarii* and the ostracod *Cyprideis torosa* may occur in the underlying in-situ muddy deposits. Additionally, micro-ripup clasts, abundant shell debris as well as edged mineral grains testify to an abrupt event-related input of both marine and terrigenous material. Post-sedimentary corrosion and pyrite formation further prove that micro- and macrofauna shells became, soon after deposition, subject to anoxic conditions typical of quiescent water bodies with restricted circulation. Fossil analysis of sample 2 shows that, in this phase of the inflow, the number of marine species decreased; however, the mixed occurrence of fully marine species (e.g. Echinoidea, *Rosalina* sp., *Urocythereis margaritifera*), freshwater indicators (*Candona neglecta*) and abundant sand and fragmented marine shells clearly documents abrupt high-energy influence. In sample 1, only *Cyprideis torosa* was encountered. We assume that the uppermost 40 cm of this fairly well sorted sand were relocated shortly after the event and re-deposited in a limnic to slightly brackish environment (see Section 4.1).

Thin sections of selected sediment samples from cores of transects A and B are depicted in Figs. 5 and 6, the position of each section being also marked in Figs. 3 and 9. At site ANI 11, a sample from autochthonous mud deposited under limnic conditions (Fig. 5c) shows prevailing silt and clay with dispersed organic matter and very few shell fragments of indeterminable species. In contrast, the upper part of the allochthonous high-energy unit (Fig. 5b) is made up of fine sand and abundant foraminifers, encountered as whole specimens and fragments. Numerous macrofossil shell remains are adjusted horizontally thus indicating palaeo-flow direction. A third sample out of weathered sandy deposits from a younger event (Fig. 5a) reveals abundant angular quartz grains, fairly unsorted and void of carbonate. Similar characteristics were found for a carbonate nodule out of a weathered event layer encountered in nearby core ANI 25 (Fig. 5e). Another sample from an older event at the same site revealed exactly the same sedimentary structure but also abundant marine shell debris and a fragment of an echinoid spine (Fig. 5f, lower left). The overall angular shape of the mineral grains reflects that rounding processes in the

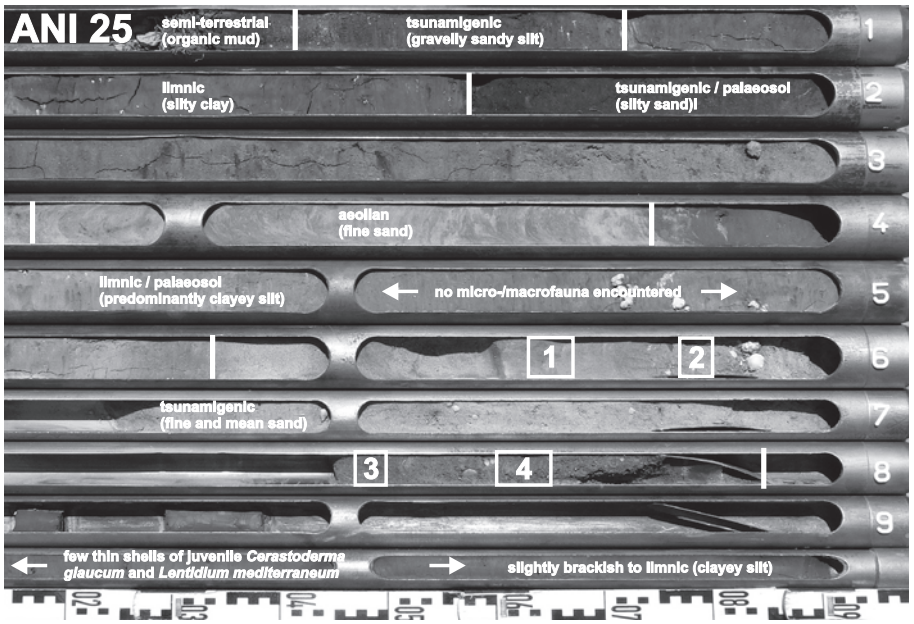

Samples 3 (ANI 25 MH 3, 6.38-6.35 m b.s.l.) and 4 (ANI 25 MH 4, 6.53-6.48m b.s.l.)
abundant quartz grains and chert fragments, cemented sand grains; silty ripup clasts; little fine organic material; abundant shell debris (debris layer), molluscs fagments mostly angular and partly corroded and/or dyed grey (esp. sample 4), covered with brass-coloured pyrite crystals; abundant foraminifers and ostracods, partly covered with black pyrite crystals

3 + 4

Gastropods
Bittium latreillii
Retusa sp.
Rissoa sp.
Turbonilla sp.

Bivalves
Acanthocardia paucicostata
Cerastoderma glaucum
Lentidium mediterraneum
Loripes lacteus
Nucula sp.
Parvicardium sp.
Tellina sp.
Venus sp.

Scaphopods
Dentalium sp.

Foraminifers
Ammonia beccarii
Ammonia cf. *parkinsoniana*
Cibicides lobatulus
Elphidium crispum
Elphidium minutum
Lagena cf. *sulcata*
Quinqueloculina elegans
Quinqueloculina cf. *venusta*
Planorbulina mediterranensis
Rosalina cf. *globularis*
Spiroloculina depressa
Triloculina sp.*

Ostracods
Aurila sp.
Aurila convexa
Basslerites berchoni
Callistocythere sp.
Carinocythereis cf. *carinata*
Cyprideis torosa
Cytheretta adriatica
Hemicytherura videns
Hiltermannicythere rubra
Loxoconcha bairdi
Loxoconcha gibberosa
Loxoconcha ovulata
Loxoconcha stellifera
Loxoconcha versicolor

Ostracods (continued)
Neocytherideis cf. *muelleri*
Paradoxostoma sp.
Pontocythere rubra
Semicytherura inversa
Semicytherura mediterranea
Semicytherura paradoxa
Semicytherura psila
Triebelina raripila
Urocythereis margaritifera
Xestoleberis communis
Xestoleberis dispar

Sample 2 (ANI 25 MH 2, 4.68-4.65 m b.s.l.)
abundant quartz grains and chert fragments; abundant shell debris and gastropod fragments, abundant caps of snail-shells, mollusc fragments mostly angular

2

Gastropods
Alvania sp.
Pirenella conica
fragments of limnic species

Bivalves
Cerastoderma glaucum
Loripes lacteus
Ostrea sp.
(cemented to fragments of limnic gastropods)

Echinoidea
Echinoid spine fragments

Foraminifers
Ammonia beccarii
Elphidium minutum
Rosalina sp.

Ostracods
Candona neglecta
Cypridopsis sp.

Ostracods (continued)
Iliocypris sp.
Loxoconcha bairdi
Loxoconcha cf. *ovulata*
Neocytherideis cf. *muelleri*
Pontocythere rubra
Semicytherura paradoxa
Semicytherura sulcata
Urocythereis margaritifera
Xestoleberis margaritifera

Sample 1 (ANI 25 MH 1, 4.55-4.51 m b.s.l.)
angular quartz grains and chert fragments; few caps of snail-shells, no organic material

1

Ostracods
Cyprideis torosa

Fig. 4. Simplified facies profile of vibracore ANI 25 drilled to the east of the Aghios Nikolaos bedrock sill and results of macro- and microfaunal analyses of sediment samples 1–4.

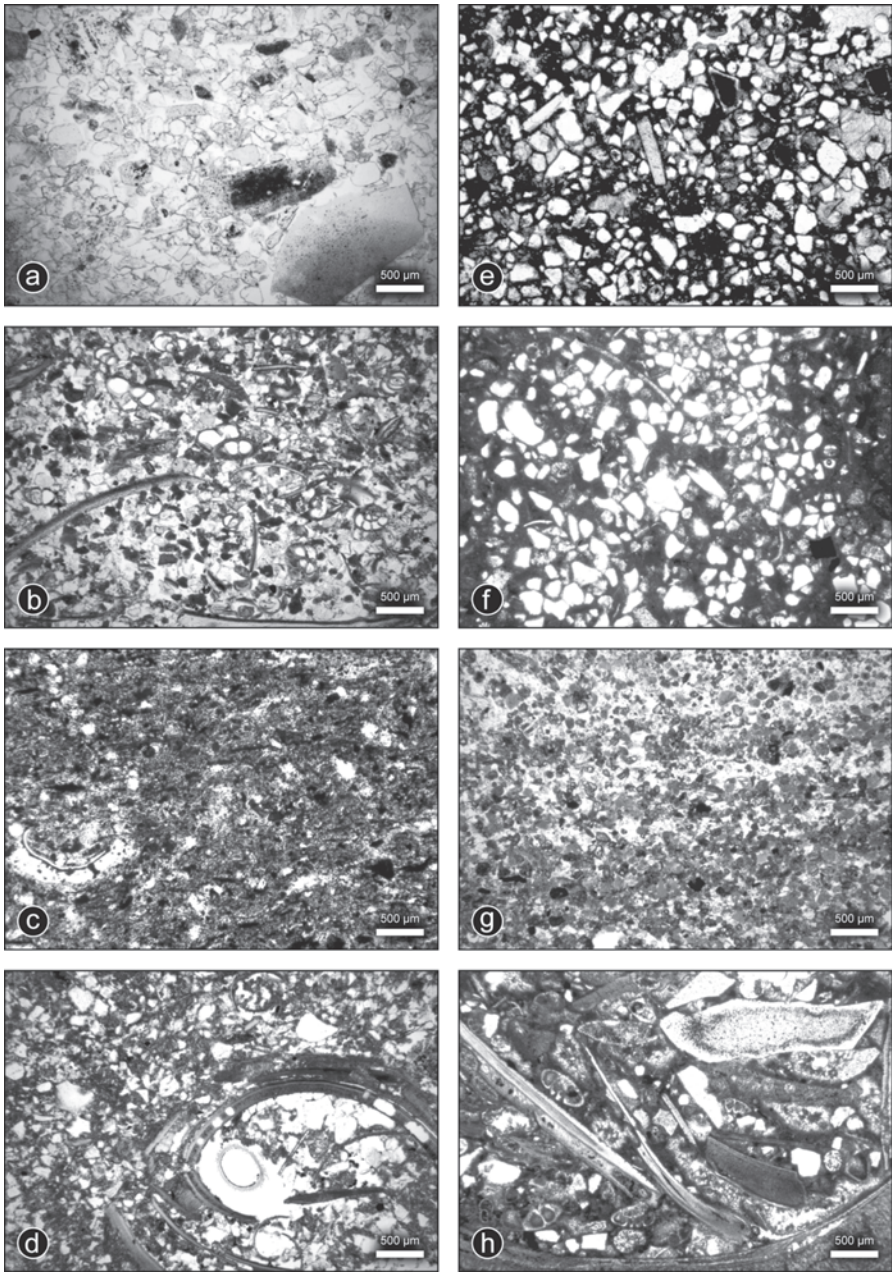

Fig. 5. Thin sections of sediment samples from vibracores drilled around the Lake Voulkaria, part I. See Figs. 1 and 2 for location of vibracoring sites, Fig. 3 for stratigraphic position of thin sections, and text for further explanations. All thin sections seen under plain polarized light. (a) ANI 11/11+ (0.70–0.65 m b.s.l.), (b) ANI 11/19+ (2.25–2.20 m b.s.l.), (c) ANI 11/26+ (5.20–5.25 m b.s.l.), (d) ANI 10/8+ (1.80–1.78 m b.s.l.), (e) ANI 25/7 KK (1.73 m b.s.l.), (f) ANI 25/17+ KK (4.79 m b.s.l.), (g) PAL 6/18+ (4.70–4.66 m b.s.l.), (h) PAL 15/16 M/KK (3.87 m b.s.l.).

source zone of the sediment were of minor importance and/or that a considerable amount of terrigenous material was incorporated. Individual findings of *Globigerina*-type foraminifers in the same sample indicate influence from the open-sea pelagic zone.

Thin sections of carbonate nodules from the oldest generation of allochthonous marine sand found in cores ANI 26 and 27 clearly testify to event-related deposition. A typically unsorted mixture of fragments of marine bivalves and gastropods, foraminifers, partly showing strong corrosion features, and edged mineral grains was found for ANI 26 (Fig. 6a and 6b). Foraminifer species such as *Textularia* sp. (Fig. 6a, left center) document fully marine conditions in the source area of the material. Postsedimentary recrystallization partly produced secondary carbonate moulds of foraminifer specimens (Fig. 6b, left center). Another sample revealed angular mineral grains up to > 1 mm associated with foraminifers such as *Ammonia beccarii* (Fig. 6c, lower left) and echinoid spine fragments (Fig. 6c, lower center) also indicating high-energy impact from a seaward direction. ANI 27 thin sections illustrate differences between autochthonous mud (Fig. 6h), overlying allochthonous shell debris (Fig. 6e-6g) and a following stratum rich in carbonate concretions (Fig. 6d). By the event, pieces of ex-situ and well rounded gravel together with macrofaunal marine shell debris and foraminifers were pressed into in-situ mud (Fig. 6h). The shell debris shows a chequered mixture of fragments of gastropods (Fig. 6g, lower left), bivalves (Fig 6f, *Cerastoderma glaucum*, upper right) and echinoids (Fig. 6f, lower left) as well as abundant specimens of foraminifers that are partly encrusted by carbonates (Fig. 6h, upper left). The dissolution structure in Fig. 6f (center) possibly corresponds to crab pincers, Fig. 6e shows a large part of an irregular sea urchin associated with few intermixing sand grains. The carbonate nodules following above consist of recrystallized carbonate; a younger generation of fissures was healed by larger carbonate crystals (Fig. 6d). We assume that the secondary carbonate comes from dissolution of primary biogenic carbonate from shell debris originally mixed with the overlying sand. Such weathered sand sections were encountered in cores ANI 11 and 26 above and around present mean sea level (see Fig. 3).

In summary, micro- and macrofossil assemblages and thin section analyses suggest that the allochthonous material making up the event layers comes from the littoral and foreshore area of a fully marine environment. At the same time, edged mineral grains show that also terrigenous material was incorporated. After subaerial deposition, intense decalcification took place; secondary carbonate subsequently precipitated in lower sections and, in some cases, fossilized original faunal assemblages. When deposited under water, marine shell fragments partly became subject to corrosion and pyrite formation due to anoxic conditions in the re-established quiescent environment.

4.3 *Subground investigations by earth resistivity tomography (ERT) and ground penetrating radar (GPR)*

Earth resistivity measurements were carried out along a SSW-NNE-running transect across Cleopatra's Canal using an electrode spacing of 4 m (Figs. 2 and 7). The processed model resistivity section reveals highest values for bedrock units in the deeper subground and for the stone bridge used to cross the canal. The bedrock units show a steplike decrease in elevation which seems to reflect a system of WNW-ESE-trending normal faults that can also be discerned in satellite images (Fig. 1). The bedrock lies deepest between the canal and vibracoring site ANI 11. Here, it

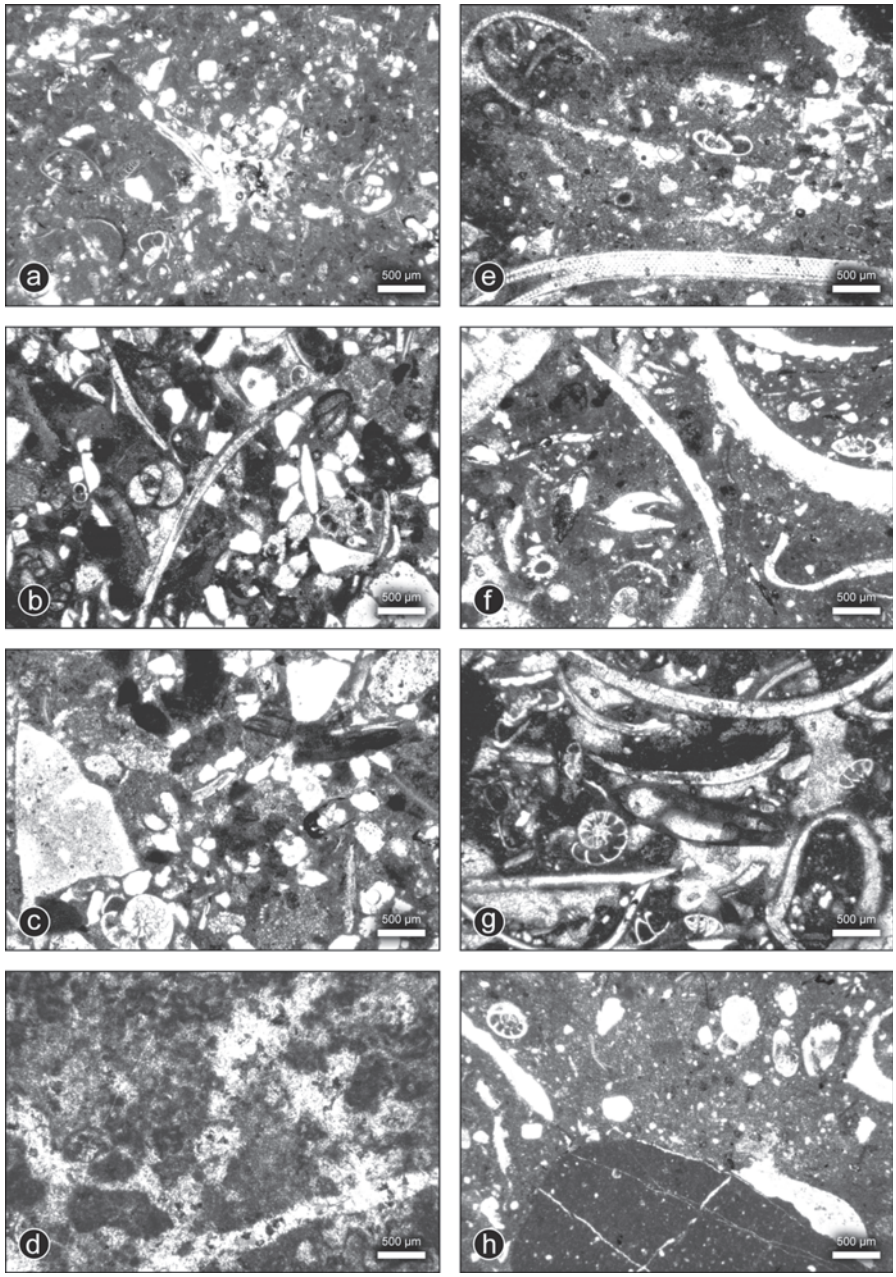

Fig. 6. Thin sections of sediment samples from vibracores drilled around the Lake Voulkaria, part II. See Figs. 1 and 2 for location of vibracoring sites, Fig. 3 for stratigraphic position of thin sections, and text for further explanations. All thin sections seen under plain polarized light apart from (d) with crossed Nichols. (a) ANI 26/21+ KK (3.76 m b.s.l.), (b) ANI 26/23 KK (4.50 m b.s.l.), (c) ANI 26/25 KK (5.20–5.15 m b.s.l.), (d) ANI 27/18 KK (3.86–3.76 m b.s.l.), (e) ANI 27/19 KK (3.93–3.89 m b.s.l.), (f) and (g) ANI 27/20 KK (4.00–3.95 m b.s.l.), (h) ANI 27/20+ KK (4.11 b.s.l.).

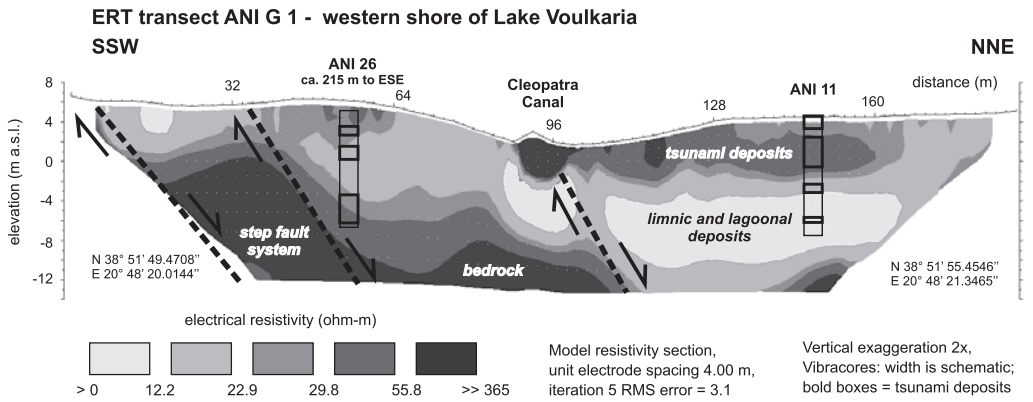

Fig. 7. Model resistivity section based on earth resistivity measurements along transect ANI G 1 across Cleopatra's Canal. See Figs. 1 and 2 for location of the transect.

is overlain by material with minimum resistivity values. Compared to the ANI 11 stratigraphy, this part of the ERT section may correspond to clayey silt (up to around 3.30 m b.s.l.) deposited in a quiescent environment. South of Cleopatra's Canal, corresponding deposits were found in greater depths (below around 6.30 m b.s.l.) but closer to the bedrock so that they are depicted less clear than on the northern side. The uppermost part of the ERT section shows increased resistivity values on either side of the canal. This is in good accordance with sandy to gravelly tsunami deposits encountered in core ANI 11, especially with those between 0.42 m b.s.l. and 2.55 m a.s.l. (Fig. 3), and similar deposits found in core ANI 26. A zone of low resistivity in the southernmost part of the ERT section might correspond to fine-grained limnic to colluvial deposits dammed by allochthonous tsunami sediments located further towards the canal.

Ground penetrating radar was applied along a WSW-ENE-running transect some 110 m to the south of coring site ANI 26 (Fig. 2). Fig. 8 depicts GPR raw data (Fig. 8a), data processed by using standard RAMAC RTA filters (Fig. 8b) and the resulting radar-stratigraphic interpretation (Fig. 8c). The topmost black horizontal continuous line or band represents the ground surface. Any other black line below corresponds to the roof of underlying layers of higher conductivity compared to the overlying strata. In Fig. 8b, four reflectors can be discerned: (i) the uppermost continuous reflector (= ground surface); (ii) a discontinuous reflector at 30 ns b.s.; (iii) a strong and continuous reflector at 40–45 ns b.s.; (iv) a discontinuous reflector at varying depths between 60–80 ns b.s. Moreover, it can be recognized that the reflectors become slightly thicker towards the ENE which may reflect thickening of the imaged strata. The lowermost reflector in Fig. 8b shows two channel-like depressions at around 50–70 m and 135–180 m distance which also delineate the deepest data imaged by the GPR transect.

Compared to the stratigraphies of cores ANI 26, 25 and 24, the latter drilled some 25 m to the east of the GPR transect (Figs. 2 and 8), the upper discontinuous reflector (30 ns b.s.) seems to correspond to weathered silty to sandy material of palaeosol P3 (Figs. 2 and 8) and the subsequent continuous reflector (40–45 ns b.s.) to palaeosol P2 consisting of clayey silt. The lowermost reflector (60–80 ns b.s.) may be consistent with the encountered stratigraphic change from thick

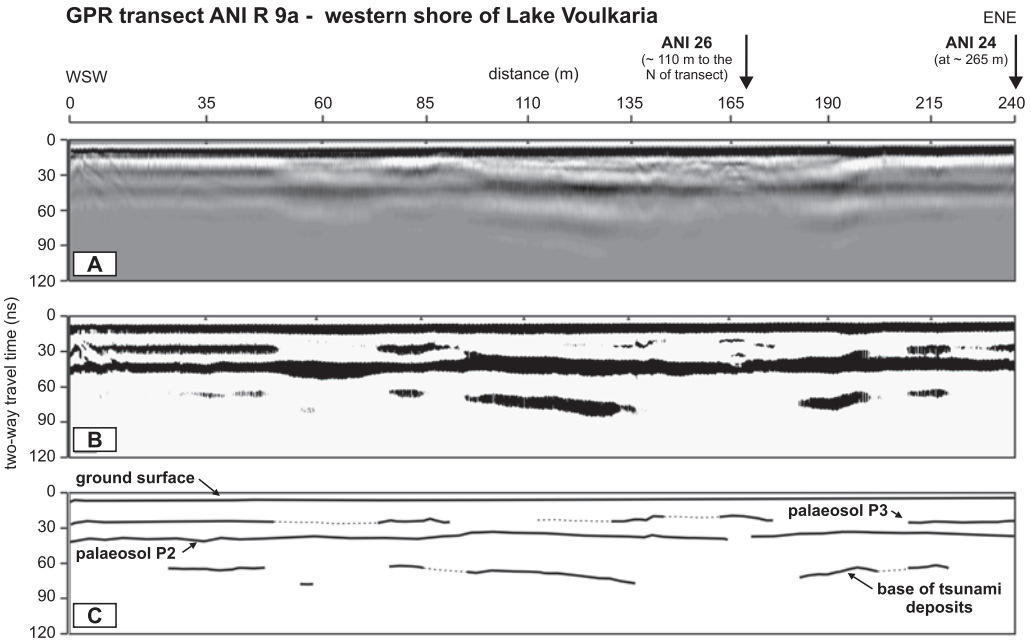

Fig. 8. Radargram along transect ANI R 9a across the western shore of the Lake Voulkaria south of Cleopatra's Canal based on measurements by ground penetrating radar. (a) raw data, (b) raw data processed by standard filters, (c) interpretation of GPR data; black lines delineate the roof of a layer characterized by higher conductivity. See Figs. 1 and 2 for location of the transect and text for further explanations.

tsunamigenic sand to underlying clayey silt accumulated in a quiescent water environment. The depressions at 50–70 m and 135–180 m distance therefore probably reflect tsunami-borne erosional channels cut into the underlying strata. This is in good agreement with erosional contacts found in cores ANI 24, 25 and 26. In general, the subparallel structure of the upper three reflectors in Fig. 8b matches well the stratigraphic similarities between cores ANI 24, 25 and 26 (Fig. 3).

5 *Event stratigraphy beneath ancient Palairos*

Vibracore transect B consists of cores PAL 6, 7 and 46 drilled on the southwestern shore of the Lake Voulkaria around 3–3.5 km away from Cleopatra's Canal and beneath the ancient city of Palairos (Figs. 1, 2 and 9).

5.1 *Sedimentary record along vibracore transect B*

Vibracore PAL 6 (0.24 m a.s.l., N 38°50'45.5'', E 20°49'49.1'') shows a thick and homogenous sequence of lacustrine clayey silt (9.78–2.73 m b.s.l.) typical of the quiescent environment of the Lake Voulkaria (Figs. 2 and 9). However, two intercalating sections revealed considerable input of allochthonous fine sand (8.56–6.54 m and especially 4.76–4.56 m b.s.l.). Thin section analysis of

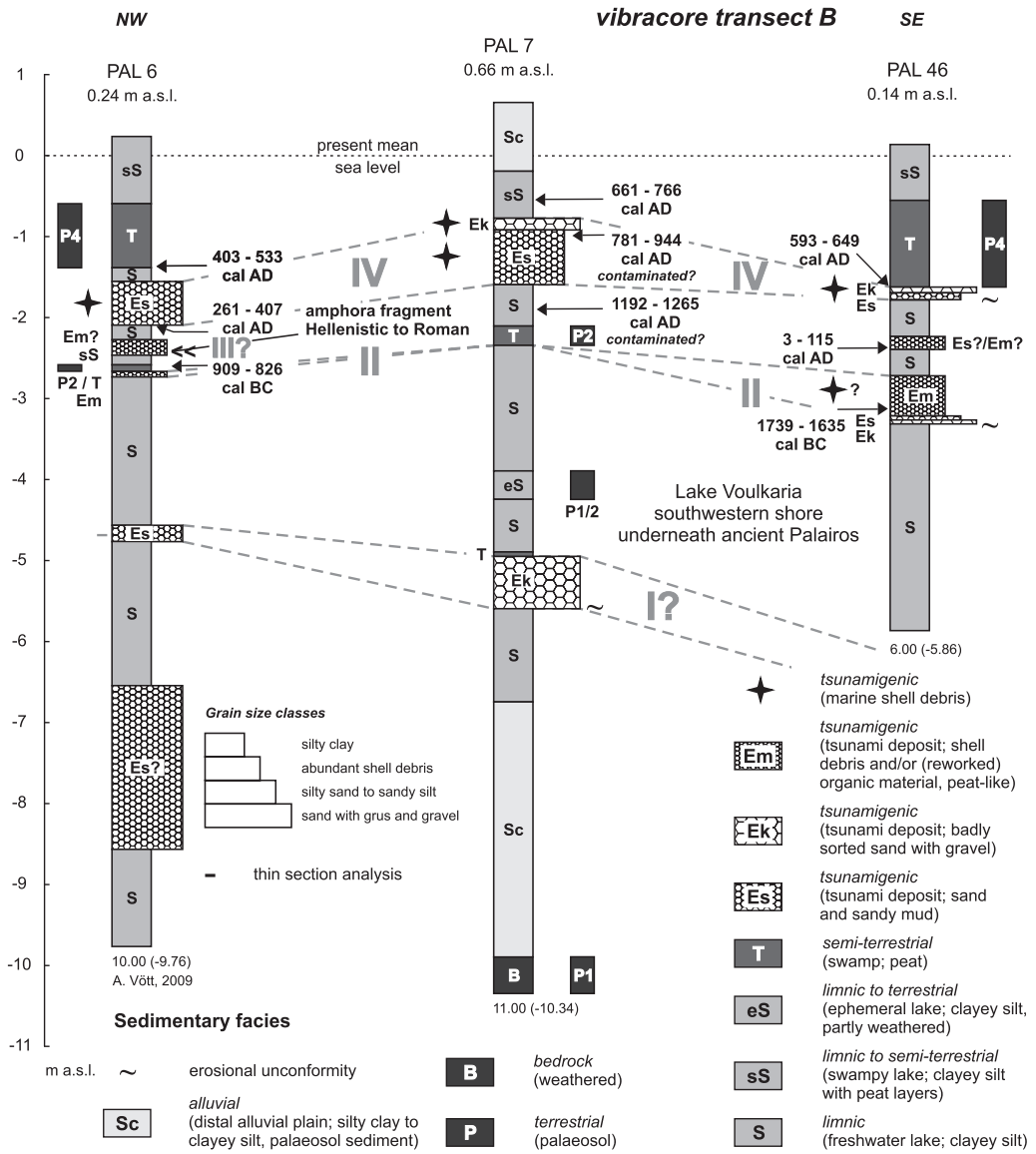

Fig. 9. Stratigraphies and vertical facies distribution for vibracores of transect B at the southwestern shore of the Lake Voulkaria (for location of transect see Figs. 1 and 2, and Fig. 12 for photos of selected vibracore sections).

the mid-core fine sand layer documents a clearly laminated structure indicating a strong water current temporarily flowing at site PAL 6 (Fig. 5g). The sediment is made up of fairly well sorted fine sand with few grains of mean sand but does not contain any macro- or microfossil remains. Further upcore, limnic deposits are repeatedly intersected, namely by a layer of large limestone fragments and partly disintegrated shell debris out of limnic molluscs (2.73–2.69 m b.s.l.), mixed and covered by strongly acidic organic material (2.69–2.58 m b.s.l.), and by a layer of sandy to silty deposits with abundant fragments of marine shells, wood and reed (2.09–1.75 m b.s.l.). An intermediary muddy layer including shell debris of most probably autochthonous species, ceramic fragments and plant remains (2.46–2.27 m b.s.l.) is less distinct and may also be due to local interferences of the sedimentary environment. Subsequently, limnic conditions were re-established (1.55–1.38 m b.s.l.), followed by peat accumulated in a swampy environment (1.38–0.59 m b.s.l.).

The base of vibracore PAL 7 (0.66 m a.s.l., N 38°50'38.7'', E 20°49'52.1'') revealed fine-grained distal alluvial fan deposits (9.89–6.74 m b.s.l.) on top of a palaeosol (Figs. 2 and 9). The following limnic sediments (6.74–2.34 m b.s.l.) are intersected by a stratum of grus and gravel with limestone fragments, up to 5 cm large, mixed with clayey silt (5.59-4.89 m b.s.l.), and a palaeosol unit (4.24–3.89 m b.s.l.). In the uppermost part of the core, we found a layer of decalcified peat (2.34–2.10 m b.s.l.) covered by again limnic (2.10–1.59 m b.s.l.) and subsequently sandy to gravelly, clearly laminated deposits including abundant marine shell debris and plant remains (1.59–0.77 m b.s.l.). The latter unit is overlain by sediments of a swampy lake which are finally covered by silty to clayey alluvial fan deposits.

Vibracore PAL 46 (0.14 m a.s.l., N 38°50'34.7'', E 20°50'02.9'') is mainly made up of homogenous lacustrine clayey silt (5.86–3.31 m b.s.l.). This unit is abruptly covered by a layer of limestone fragments, up to 5 cm in diameter, fine sand, shell debris, wood fragments and abundant remains of *Phragmites* sp. (3.31–2.84 m b.s.l.; Figs. 2 and 9). Limnic conditions were subsequently re-established (2.84–1.78 m b.s.l.), the homogenous sedimentary unit showing another but less distinct shell debris layer (2.39–2.23 m b.s.l.). The limnic sequence is finally topped by sand and gravel, partly very well rounded, with abundant marine shell debris, organic material and chert fragments, up to 2 cm large (1.78–1.62 m b.s.l.). This mixed layer is covered by peat (1.62–0.55 m b.s.l.) and subsequently by clayey silt rich in organic matter.

In a summary view, homogenous limnic sediments from the southwestern shore of the Lake Voulkaria revealed several intersecting layers of moderate to high-energy deposits out of sand, gravel, wood and plant remains and/or abundant shell debris, partly of marine origin (Fig. 9). It has to be considered that (i) the intersecting strata do not reflect the autochthonous quiescent sedimentary environment typical of the lake; (ii) strong similarities between the stratigraphies of transect B cores suggest identical evolution over a large distance (see Fig. 9) controlled by natural factors and not by man; (iii) the abrupt input of sand and gravel and marine shell debris originating from the seaside can only be explained by strong saltwater inflow across the Aghios Nikolaos bedrock sill towards a southeastern direction. This scenario goes well with the stratigraphic findings along transect A. Decreased thicknesses of allochthonous sediment layers in cores of transect B reflect longer distances to the sediment source around or west of Aghios Nikolaos and thus decreased flow energy due to diverging effects; (iv) input of coarse-grained material by local torrential systems can be excluded; coring site PAL 7 is located in the very marginal zone of an alluvial fan and sites PAL 6 and 46 are located in sheltered positions.

We thus conclude that each of the intercalating high-energy deposits documents the sudden and temporary increase in sedimentary dynamics bound to a severe disturbance of the autochthonous quiescent low-energy lake environment. Each disturbance was directly caused or, at least, indirectly initiated by tsunami influence.

5.2 *Geochemical and computer tomography approaches*

Geochemical parameters of sediment samples are useful facies indicators in stratigraphic sequences (Vött et al. 2002). In the nearby lagoonal Sound of Lefkada, high-energy event layers could be empirically traced by high Ca^{2+}/Mg^{2+} ratios (Vött et al. 2008c). For the Lake Voulkaria, we used Ca^{2+}/K^{+} ratios of cores PAL 6 and 7 in order to test the hypothesis if peaks are consistent with high-energy impact on the sites (Fig. 10). The Ca^{2+} concentration is supposed to increase with increasing saltwater influence; the K^{+} concentration is supposed to reflect more autochthonous influence (Vött et al. 2002). In cores PAL 6 and 7, the topmost event layers are indeed characterized by high Ca^{2+}/K^{+} values, in core PAL 7 also the event layer encountered at 5.59–4.89 m b.s.l. However, strong sedimentary disturbances found in similar stratigraphic positions and comparable depths in PAL 6 (2.73–2.58 m b.s.l.) and PAL 7 (2.34–2.10 m b.s.l.) are reflected by minimum Ca^{2+}/K^{+} ratios. This is because both event layers are considerably decalcified by strong acid compounds of incorporated organic material (see Section 5.1). Thus, the Ca^{2+}/K^{+} ratio is only of limited use for the complete detection of event layers in the Lake Voulkaria sedimentary record.

A one meter long section of core PAL 6 (1–2 m b.s., 0.76–1.76 m b.s.l.) was analyzed by computer tomography (Fig. 11). Both x-ray picture and density index values revealed three distinct units consistent with the PAL 6 stratigraphy (Fig. 9). The lowermost unit shows the highest relative density due to high amounts of tsunamigenic sand and shell debris with individual valves of

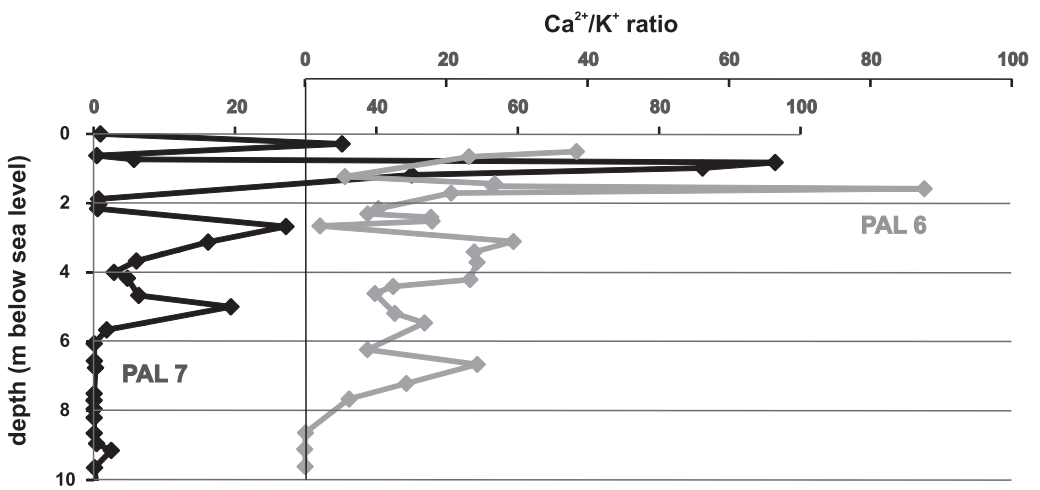

Fig. 10. Vertical graphs of the Ca^{2+}/K^{+} ratio of sediment samples from cores PAL 6 and 7 based on geochemical analyses. Note that the graph for PAL 6 is shifted to the right for better reading.

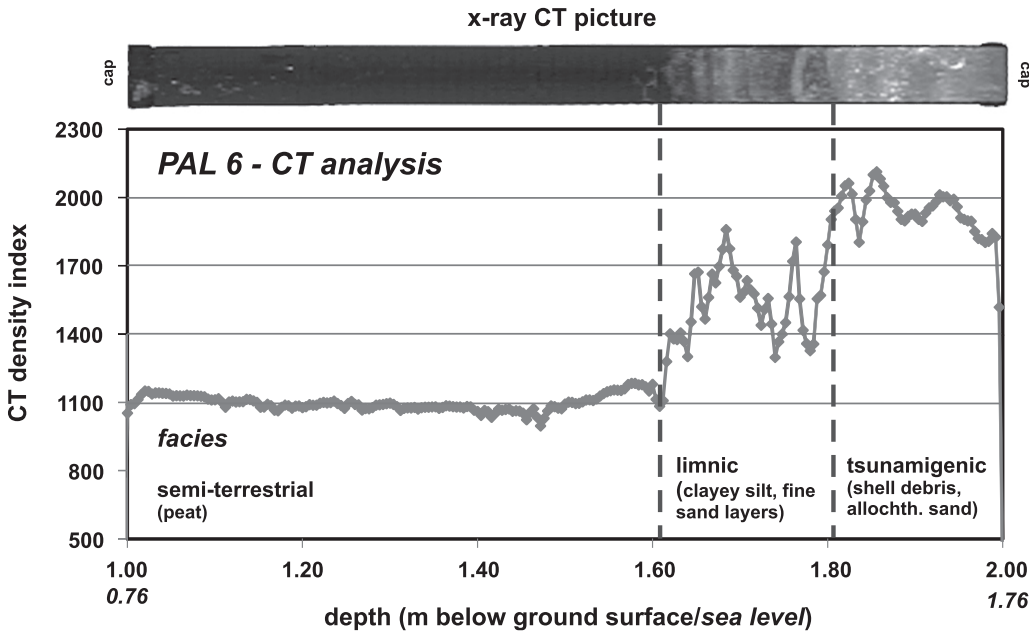

Fig. 11. Computer tomography analysis of a selected section of core PAL 6 from the southwestern shore of the Lake Voulkaria.

marine bivalves that can be discerned in the x-ray picture. Subsequently follow less dense limnic deposits with integrated thin layers of reworked fine sand bearing a clearly laminated structure. This unit is covered by peat with homogenously low density values. The presented CT section of core PAL 6 documents (i) the recovering lake environment after a strong high-energy impact, and (ii) for the first time in the record of transect A and B cores, a switch-over to the formation of a thick peat layer. The wide belt of *Phragmites* sp., presently characteristic of the Lake Voulkaria shores, did not exist before the last event that hit the lake and initiated strong eutrophication by the inflow of saltwater.

6 *Event markers in profundal and allover lakeside deposits*

Fig. 12 gives an overview of selected core sections from transects A and B as well as of further core sections from sites around Aghios Nikolaos and the shores of the Lake Voulkaria. Underwater core ANI 20 from the southeastern part of the Bay of Cheladivaron revealed more than 50 cm thick sandy to gravelly material rich in marine shell fragments abruptly covering autochthonous lagoonal deposits. Core ANI 10 shows a comparable stratigraphy but is located on the eastern side of the bedrock sill close to site ANI 7. A thick layer of ex-situ sand and gravel intersects limnic mud. An earlier event seems to be responsible for the input of fine sand at 2.69–2.62 m b.s. which was subsequently reworked and partly integrated into the limnic deposits. Vibracore ANI 46 was

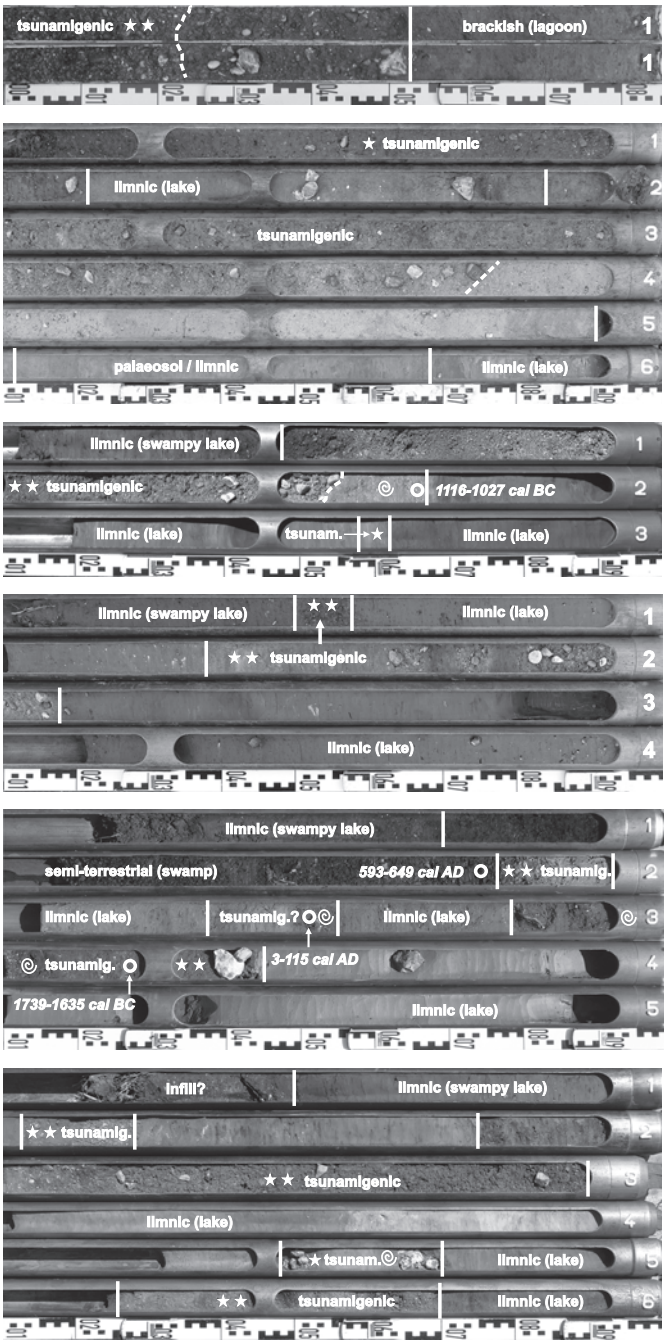

ANI 20
ground surface 0.30 m b.s.l.

Inner Bay of Aghios Nikolaos

ANI 11
ground surface 4.50 m a.s.l.

Leeward side of Aghios Nikolaos bedrock sill

ANI 10
ground surface 0.20 m b.s.l.

Western shore of Lake Voulkaria

ANI 46
ground surface 1.13 m a.s.l.

Western shore of Lake Voulkaria

PAL 46
ground surface 0.14 m a.s.l.

Southwestern shore of Lake Voulkaria

PAL 15
ground surface 0.81 m a.s.l.

Eastern shore of Lake Voulkaria

Fig. 12. Photos of selected vibracores from the shore of the Lake Voulkaria and simplified facies profiles. Note that only the uppermost sections of each profile are depicted (for locations of vibracores see Figs. 1 and 2).

drilled some 380 m to the northeast of Cleopatra's Canal on the west-northwestern shore of the Lake Voulkaria. Again, the limnic sequence shows two distinct intercalations of coarse-grained allochthonous material in the uppermost 4 m of the core. Coring site PAL 15 is located on the eastern shore of the lake just opposite to ANI 46 but some 3.7 km away. Besides two younger high-energy event deposits comparable to those from ANI 46, we encountered sediments of two earlier impacts between 4 and 6 m b.s. The PAL 15 event deposit found at 4.67–4.54 m b.s. (3.86–3.73 m b.s.l.) includes numerous fragments of marine molluscs, partly cemented to mineral grains, and well rounded pieces of gravel up to 1 cm large. Thin section analysis revealed a mixture of shell debris, foraminifers and large angular mineral grains of terrigenous origin (Fig. 5h). Event layers were also found near the southern and southeastern shores at sites PAL 3 and PAL 30.

Based on the facts that (i) coarse-grained intercalations out of allochthonous high-energy deposits were encountered both in the profundal zone of the lake and along the western (transect A), southwestern (transect B), southern (PAL 3), southeastern (PAL 30), eastern (PAL 15) and west-northwestern shores (ANI 46, see Figs. 1, 2 and 12); (ii) there are clear stratigraphic correlations between the allover lakeside event deposits; (iii) there is no evidence of marine influence across the Palairos coastal plain from the southern side (Jahns 2005, 2007, 2009, Vött et al. 2006b, 2007b), we conclude that the whole lake environment was affected by multiple tsunami impact from the seaside across the Aghios Nikolaos bedrock sill.

We determined the accumulated thickness of allochthonous coarse clastics (sand, gravel, shell debris) down to 5 m and to 8 m b.s. for 17 cores from the Lake Voulkaria area and for 2 cores from the inner Bay of Cheladivaron. Thickness was then multiplied by the elevation of the coring site (ground surface) to get a rough approximation of the energy needed for moving the sediment masses. Fig. 13 illustrates energy figures with respect to 5 m and 8 m depth below surface. Highest energy figures were found for the area east of the bedrock sill showing that maximum energy was needed to cross or even break through the sill. Older generations of high-energy impact (differences of energy figures for accumulated thickness down to 8 and 5 m b.s.) seem to have predominantly affected the western, southern and eastern shores of the Lake Voulkaria. In contrast, younger generations (energy figures for accumulated thickness down to 5 m b.s.) concentrated on the western and southwestern shores probably in the form of strong water currents flowing along the foot of Mt. Asprochorto (275 m a.s.l.) in a southeastern direction (see Fig. 2).

7 *Dating tsunami impact on Lake Voulkaria*

Dating tsunami deposits by means of radiocarbon measurements and age determination of diagnostic ceramic fragments is problematic unless (i) the dating samples are taken from underlying pre- and/or overlying post-tsunami deposits (sandwich strategy) so that reworking effects can be excluded, (ii) erosion of the pre-tsunami base is negligible and (iii) tsunami deposits were covered by younger sediments including dating material and thus were not subject to subaerial weathering.

In this paper, we present 13 new radiocarbon dates, 4 dates already published by Vött et al. (2006a) and 12 dates from Jahns (2005) that were re-evaluated and recalibrated. Radiocarbon dating results are summarized in Table 1. Age inversion occurred for samples from core PAL 7 possibly due to contamination. Pollen analysis was conducted for 12 sediment samples from core ANI 24.

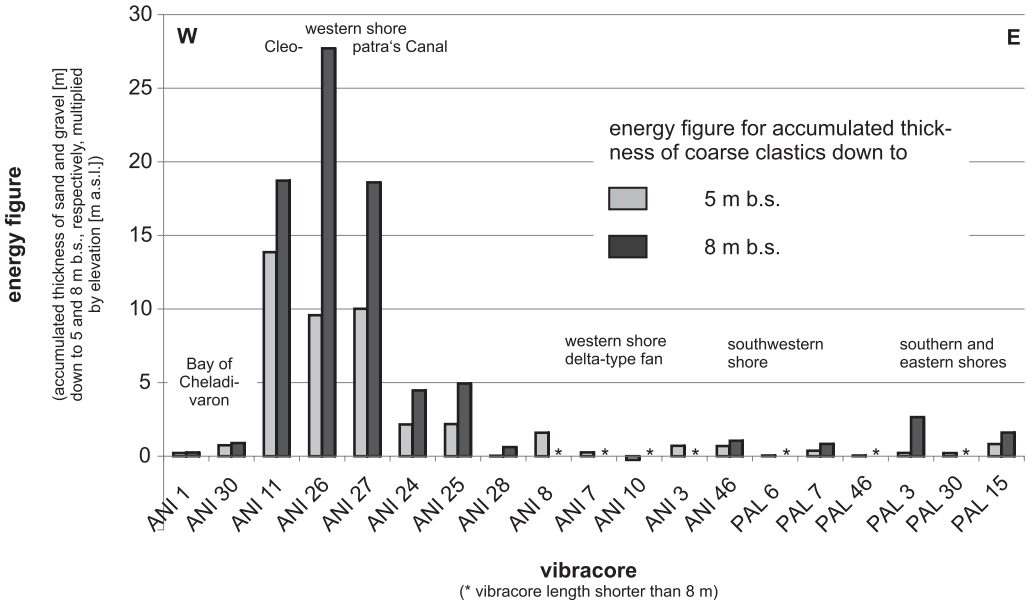

Fig. 13. Energy figures for 19 cores from the inner Aghios Nikolaos Bay and the shores of the Lake Voulkaria based on the accumulated thickness of coarse-grained sediments down to 5 m and 8 m b.s. in relation to ground surface elevation. See Figs. 1 and 2 for locations of vibracores and text for further explanations.

The main objective was to detect possible correlations with the high-resolution pollen diagram of Jahns (2005, 2007, 2009) for core VOUL 1 from the center of the lake. We refrained from pollen type differentiation within the plant family *Oleaceae* (here comprising *Olea* sp. and *Phillyrea* sp.) as this would have required time-consuming measurements of the thickness of the pollen grain wall (*Olea* sp: 3.0–3.2 µm; *Phillyrea* sp.: 1.4–2.0 µm; see Punt et al. 1991, Beug 2004). Detailed counting of both species is already available for core VOUL 1. Few geoarchaeological findings were found useful to date palaeoenvironmental changes in the environs of the Lake Voulkaria.

8 *Discussion*

Establishing a local tsunami geochronology

Along transect A across the Aghios Nikolaos bedrock sill, repeated interferences of autochthonous sedimentary conditions were found in the individual vibracores (Fig. 3) Strong stratigraphic correlations exist between cores ANI 24 to 27 and, at least in the upper section of the core, ANI 11. These profiles show three intercalating layers of coarse-grained material each of them with a palaeosol on top (P2 to P4). However, determining stratigraphic correlations between these central cores of transect A on the one hand, and cores ANI 1, ANI 7, and VOUL 1 from the inner Aghios Nikolaos Bay, the western shore, and the profundal zone of the Lake Voulkaria on the

other hand, is problematic. This is mostly due to considerable differences in the grade of weathering. Only the youngest generation of coarse-grained sediments can be easily traced all across the sill because of its strikingly high content of large chert fragments (Fig. 3).

Based on reliable stratigraphic correlations and age control by radiocarbon dates and the results of palynological analyses, four different generations of tsunami impact were classified for transects A and B.

Tsunami generation I

Tsunami generation I deposits, post-dated to the 6th millennium BC, were only found in the inner Bay of Aghios Nikolaos at site ANI 1. Here, this strongly transgressive impact hit a former freshwater lake environment and, by connecting the lake to the marine system, induced saltwater conditions still prevailing in our times (Fig. 3). Similar traces of early mid-Holocene tsunami influence were found in the nearby Lagoon of Lefkada (Vött et al. 2008c). However, correlating age-controlled traces of sudden high-energy impact were not detected for the Lake Voulkaria and its shores. As for transect B, allochthonous deposits encountered around 5 m b.s.l. in cores PAL 6 and 7 (Fig. 9) could stratigraphically correspond to generation I deposits.

Tsunami generation II

Along transect A, sedimentary evidence of tsunami impact was found in cores ANI 7, ANI 10 and in core VOUL 1 (Fig. 3) consistently dating to the time around 1000 cal BC (generation II). It is a matter of discussion whether the lowermost allochthonous high-energy deposits of cores ANI 24 to 27 correspond to this generation: Plant remains from limnic sediments of core ANI 11 yielded a radiocarbon age of 45590 ± 1070 conv ^{14}C BP indicating an unknown age beyond the range of the radiocarbon method (ANI 11/27 GPRA, Table 1). Provided that there is a stratigraphic correlation with the fine-grained autochthonous and partly saltwater-influenced deposits from the bases of cores ANI 24 to 27, this would mean an interglacial age of these deposits and possibly also of the overlying allochthonous material. This is contrary to the interpretation of palynological data from the lower section of core ANI 24 which we conducted for relative dating for lack of appropriate samples for radiocarbon age determination. Samples analyzed from core ANI 24 comprised sediments between 11.85–7.50 m b.s. (11.01–6.66 m b.s.l.) from limnic and slightly brackish environments as well as allochthonous high-energy deposits.

The resulting ANI 24 pollen diagram was compared to the detailed pollen profile published by Jahns (2005, 2007, 2009) for VOUL 1. Results and interpretation are summarized in Fig. 14. Our interpretation is based on the following observations. (i) Pollen diagram ANI 24 depicts a pollen spectrum typical of interglacial vegetation dominated by trees; (ii) diagram ANI 24 is in good accordance with diagram VOUL 1 and thus seems to reflect a section of the Holocene vegetation history; (iii) compared to the chronostratigraphy of Jahns (2005), diagram ANI 24 covers the time span between around the 6th millennium BC (base) and the end of the 2nd millennium BC (top); our main arguments are given as follows: (a) Strong decrease of *Poaceae* sp. pollen found by Jahns (2005) for the time until around 5208–5021 cal BC (ANI 24: samples 28–26, Fig. 14);

Table 1. Radiocarbon dates of samples from the western and southwestern shores of Lake Voulkaria and the environs of Aghios Nikolaos.
Note: b.s. – below ground surface; b.s.s. – below sediment surface; b.s.l. – below sea level; a.s.l. – above sea level; b.l.l. – below lake level (samples marked by #); *Cerastoderma gl.* – *Cerastoderma glaucum*; artic. spec. – articulated specimen; * – marine reservoir correction with 402 years of reservoir age; 1σ max; min cal BP/BC (AD) – calibrated ages, 1σ-range; ";" – there are several possible age intervals because of multiple intersections with the calibration curve; Lab. No. – laboratory number, Beta Analytic (Beta), University of Erlangen (Erl), University of Kiel (Kia), University of Utrecht (UtC); # – recalibrated and re-evaluated radiocarbon dates published by Jahns (2005) using the Calib 5.0.2. software (see Hughen et al. 2004; Reimer et al. 2004).

Sample Name	Depth (m b.s./b.s.s.)	Depth (m b.s.l./ b.l.l.)	Sample Description	Lab. No.	$\delta^{13}C$ (ppm)	^{14}C Age (BP)	1σ max; min (cal BP)	1σ max; min (cal BC)
ANI 1/7 M	2.59	2.53	*Dosinia exoleta*, artic. spec.	UtC 13677	-1.7	5977 ± 47	6437 - 6321	4488 - 4372*
ANI 1/22 PR	8.37	8.31	peat	UtC 13676	-27.9	7040 ± 41	7933 - 7844	5984 - 5895
ANI 2/16++ PR	10.28	10.00	sea weed remains	Erl 9794	-14.4	1499 ± 40	1101 - 984	849 - 966 AD*
ANI 7/14 PR	2.30	2.20	wood fragment	Erl 9051	-25.2	2278 ± 48	2347; 2182	398; 233
ANI 7/15+ PR	2.43	2.33	unidentified plant remains	Erl 9052	-17.4	2786 ± 48	2952; 2805	1003; 856
ANI 10/9+ PR	1.67	1.87	unidentified plant remains	Kia 28882	-13.0	2890 ± 25	3065; 2976	1116; 1027
ANI 11/27 GPRA	9.80	5.30	unidentified plant remains	Beta 253821	-25.8	45590 ± 1070	–	–
ANI 14/7+ PR	3.53	2.89	sea weed remains	Kia 31664	-13.8	1590 ± 29	1202 - 1117	748 - 833 AD*
PAL 6/3+ PR	1.60	1.36	peat	Erl 9814	-26.1	1614 ± 46	1547 - 1417	403; 533 cal AD
PAL 6/7+ PR	2.34	2.10	fragments of *Phragmites* sp.	Erl 9815	-23.0	1693 ± 41	1689; 1543	261; 407 cal AD
PAL 6/11+ PR	2.84	2.60	peat	Erl 9816	-23.5	2727 ± 46	2858 - 2775	909 - 826
PAL 7/2+ PR	1.20	0.54	peat	Erl 9817	-26.4	1312 ± 38	1289; 1184	661; 766 cal AD
PAL 7/6 PR	1.65	0.99	unidentified plant remain, wood	Erl 9818	-27.5	1162 ± 41	1169; 1006	781; 944 cal AD
PAL 7/8 R	2.55	1.89	unidentified plant remain	Erl 9819	-25.8	812 ± 39	758; 685	1192; 1265 cal AD
PAL 46/2+ PR2	1.75	1.61	peat	Beta 253818	-22.1	1440 ± 40	1357 - 1301	593 - 649 AD
PAL 46/6 PR	2.52	2.38	remains of *Phragmites* sp.	Beta 253819	-19.9	1950 ± 40	1947; 1835	3; 115 AD
PAL 46/8+ PR	3.27	3.13	remains of *Phragmites* sp.	Beta 253820	-25.0	3390 ± 40	3688; 3584	1739; 1635
Kia 12857#	7.46	10.56	pollen	Kia 12857	-31.0	8806 ± 46	10108; 9704	8159; 7755
Kia 12854#	7.46	8.99	pollen	Kia 12854	-32.6	6146 ± 66	7157 - 6970	5208 - 5021
Kia 12853#	4.66	7.76	pollen	Kia 12853	-29.8	4693 ± 38	5567; 5325	3618; 3376
Kia 12852#	3.38	6.48	pollen	Kia 12852	-28.9	3197 ± 50	3460 - 3373	1511 - 1424
Kia 10322#	3.13	6.23	leaf blade of Poaceae	Kia 10322	-13.3	2784 ± 39	2948 - 2846	999 - 897
Kia 17102#	2.90	6.00	shells of limnic molluscs	Kia 17102	-5.5	2650 ± 25	2770 - 2749	821 - 800
Kia 12851#	2.70	5.80	pollen	Kia 12851	-19.3	2475 ± 51	2705; 2469	756; 520
Kia 17101#	2.64	5.74	fragments of *Cerastoderma gl.*	Kia 17101	-1.7	2565 ± 25	2298 - 2198	349 - 249*
Kia 17100#	2.22	5.32	fragments of *Cerastoderma gl.*	Kia 17100	-3.3	2515 ± 25	2247 - 2137	298 - 188*
Kia 9914#	1.98	5.08	pollen	Kia 9914	-30.2	1919 ± 150	2046; 1634	97 cal BC; 316 cal AD
Kia 17103#	1.74	4.84	fragments of *Cerastoderma gl.*	Kia 17103	-3.8	2245 ± 25	1886 - 1812	64 - 138 cal AD*

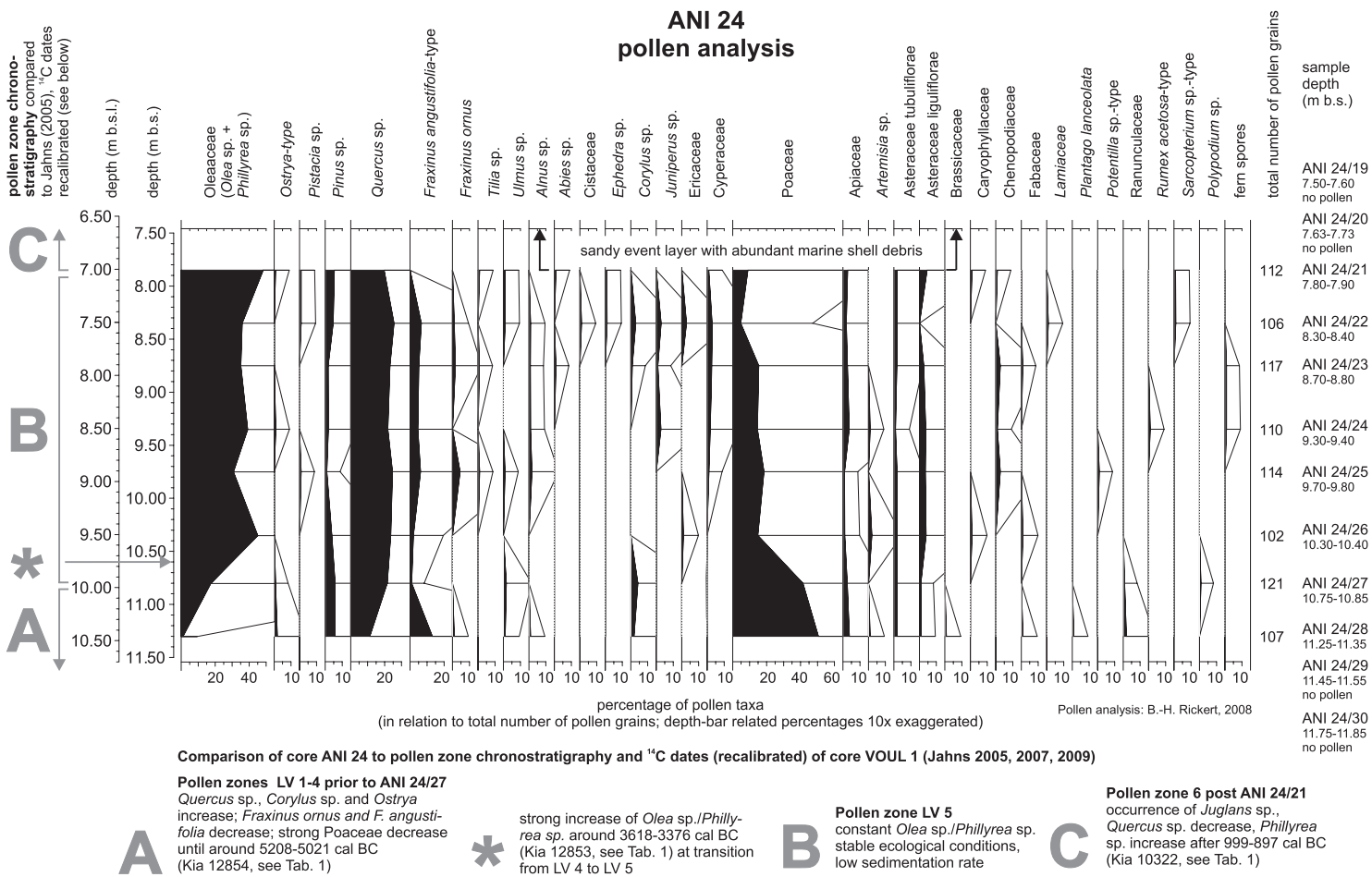

Fig. 14. Pollen diagram for the western shore of the Lake Voulkaria based on sediment samples from vibracore ANI 24. See text for further explanations.

(b) strong increase of *Oleaceae*-type pollen dated by Jahns (2005) to 3618–3376 cal BC (ANI 24: sample 26) and subsequently stable ecological conditions persisting for a long time (ANI 24: samples 26–21); (c) the lack of *Juglans* sp. pollen found by Jahns (2005) for the time before 999–897 cal BC (no *Juglans* sp. pollen in studied ANI 24 sediments). Based on these results, the sandy event layer abruptly covering Lake Voulkaria mud in core ANI 24 at 7.75 m b.s. (6.91 m b.s.l.) seems to correspond to the 'Brown Layer' of core VOUL 1. This would mean that the lowermost coarse-grained allochthonous deposits encountered in cores ANI 24 to 27 correspond to tsunami generation II from around 1000 cal BC (Fig. 3). Moreover, microfaunal analyses of corresponding material from core ANI 25 did not yield any evidence of a last interglacial age (Fig. 4). Final answers to this discussion could be given by OSL dating approaches of the event sediment itself so that potential reworking effects can be excluded. Even in case of a pre-Holocene age, however, the general nature of the deposit remains the same, i.e. the one of a high-energy tsunami impact.

Based on palynological and microfaunal analyses, it may so far be suggested that layers of allochthonous sand and gravel encountered on both sides of Cleopatra's Canal can be parallelized with tsunami generation II. The fact that tsunami deposits and underlying quiescent water deposits at sites ANI 24 to 26 lie comparatively deeper than possibly corresponding deposits encountered in cores ANI 7, 11, 27 and VOUL 1 can be explained by strong subsidence and sediment compaction due to the sedimentary load of tsunami layers that revealed to be thickest on the southern side of Cleopatra's Canal. In central transect A, abundant reworked tsunami material was deposited in a shallow water limnic environment, the sediments of which subsequently became subject to subaerial weathering and soil formation (P2 palaeosol in Fig. 3).

Concerning transect B, peat covering an event marker found at 2.73–2.69 m b.s.l. in core PAL 6 was dated to 909–826 cal BC (PAL 6/11+ PR, Table 1, Fig. 9). As for core PAL 46, remains of reed (*Phragmites* sp.) encountered in a mixed layer out of limestone fragments, fine sand, shell debris and organic material yielded an age of 1739–1635 cal BC (PAL 46/8+ PR, Table 1). Strong stratigraphic and sedimentary similarities between tsunamigenic layers at coring sites PAL 6, 7 and 46 suggest that these event layers were deposited by the same event. Based on the possibly reworked nature of the dated *Phragmites*-remains from PAL 46, the post-tsunami date given for PAL 6 is assumed to be more precise; thus, the high-energy layers can be affiliated to tsunami generation II dated to around 1000 cal BC for transect A.

Tsunami generation III

Based on stratigraphies and radiocarbon dates found for cores ANI 7 and VOUL 1 (Fig. 3, Table 1), corresponding layers of allochthonous deposits were grouped into a younger generation of tsunami impact (III). A wood fragment from the base of allochthonous marine sand encountered at site ANI 7 at 2.33–1.77 m b.s.l. was dated to 398–233 cal BC (ANI 7/14 PR, Table 1). This age goes well with the date obtained for the sudden change towards saltwater-influenced conditions detected in core VOUL 1 (349–249 cal BC, Kia 17101, Table 1, see Jahns 2005, Vött et al. 2006a). However, both ages represent maximum ages. In transect B, we found intermediary shell debris layers intersecting limnic deposits at sites PAL 6 (2.46–2.27 m b.s.l.) and PAL 46 (2.39–2.23 m b.s.l., Fig. 9) in a corresponding stratigraphic position. However, they are less distinct than layers out of

allochthonous material encountered further above and below; also, corresponding sediments were not encountered in core PAL 7 which may rather indicate more local disturbances of the environment than a tsunami impact. In vibracore PAL 6, a diagnostic ceramic fragment embedded in this mixed layer of shell debris and plant remains yielded a Hellenistic to Roman maximum age for the time of deposition. In core PAL 46, remains of *Phragmites* sp. were dated to 3–115 cal AD (PAL 46/6 PR, Table 1). Although maximum ages of transect A cores have to be considered with care, it cannot be definitely excluded that the intermediary signatures found in cores PAL 6 and PAL 46 are due to the same event than the one detected in cores ANI 7 and VOUL 1, so that a Classical-Hellenistic to maximum Roman age seems most plausible for deposits of tsunami generation III. By previous studies, strong tsunami influence on the Bay of Aghios Nikolaos was found for the time between 395–247 cal BC based on various sedimentological and geoarchaeological findings (Vött et al. 2008b).

The partly weathered allochthonous sandy deposits encountered in cores ANI 24 to 27 and ANI 1, subsequently weathered to palaeosol P3, possibly represent corresponding event deposits. Unfortunately, there is no age control for this assumption.

Tsunami generation IV

The youngest generation of tsunami deposits found in transect A cores can be easily identified, correlated and distinguished from older event deposits by its strikingly high content of chert fragments, up to 3 cm in diameter (Figs. 3 and 12).

Close to transect A, remains of a building (Daux 1960) or of bridge pylons (pers. comm. Melisch 2005) from Roman times are located some 90 m to the SE of coring site ANI 11 (Fig. 3). Taking into account that the remains lay at between 1.5 (base) and 3.5 m a.s.l. (top) on top of an artificial terrace near the excavated modern canal, it seems that they were embedded or at least partly covered by tsunami generation IV deposits encountered at nearby coring site ANI 11 between 0.73–2.55 m a.s.l. The tsunami generation IV can thus be dated to Roman or post-Roman times.

Youngest tsunami influence in transect B cores can be time-bracketed (i.e. pre- and post-dated) by PAL 6 radiocarbon ages to have occurred between 261–407 cal AD and 403–533 cal AD (PAL 6/7+ PR and PAL 6/3+ PR, Table 1, Fig. 9). Radiocarbon dates obtained for core PAL 7 show strong age inversion possibly due to contamination; we suggest that the uppermost age is the most reliable and thus exclude the two lower ones from further consideration. The youngest PAL 7 event layer thus dates to the time before 661–766 cal AD (PAL 7/2+ PR, Table 1). A sample from the base of the peat layer overlying tsunamigenic sand, gravel and marine shell debris in core PAL 46 yielded an age of 593–649 cal AD (PAL 46/2+ PR2, Table 1). This date is in overall accordance with dates obtained for PAL 6 and PAL 7. Radiocarbon ages for the youngest tsunami generation encountered in cores of transect B are also consistent with geoarchaeological age control around transect A. We thus conclude that these deposits belong to the same tsunami generation IV.

Former studies revealed multiple tsunami impact on Actio Headland and the Bay of Aghios Nikolaos (Vött et al. 2006a, 2007a, 2008b, 2008c, 2008d, 2008e, May et al. 2007). Based on radio-

carbon dates of two sea weed samples from cores ANI 2 and ANI 14, a young tsunami generation was dated to around 840 cal AD (Vött et al. 2007a). Age calibration was made using an average marine reservoir effect of 402 years assuming that sea weed incorporates old ^{14}C atoms. However, this is a matter of discussion all the more as the real local reservoir effect during the lifetime of the organism may have strongly differed from the given 402 years (Reimer & McCormac 2002, Geyh 2005). Therefore, we prefer in this case to compare conventional ^{14}C dates as follows. Samples PAL 6/3+ and ANI 14/11+ pre-date young tsunami influence to 1693 ± 41 conv BP and 1590 ± 29 conv BP, respectively, while samples PAL 6/7+ and ANI 2/16++ post-date the event to 1614 ± 46 conv BP and 1499 ± 40 conv BP, respectively (BP = 1950 cal AD, see Table 1). This comparison shows that the given dates for tsunami impact are pretty well consistent. Thus, Lake Voulkaria generation IV deposits seem to have correlative deposits in the outer Bay of Aghios Nikolaos. Considering that (i) the Lake Voulkaria represents an outstanding tsunami sediment trap enabling to distinguish between different generations of allochthonous sandy to gravelly tsunami deposits and autochthonous muddy sediments way better than the littoral system to the west and that (ii) the Lake Voulkaria radiocarbon ages are not subject to problematic marine reservoir effects, *calibrated* PAL 6, 7 and 46 ages for the tsunami generation IV have to be preferred instead of younger calibrated ages for the same event based on problematic reservoir effect correction (Vött et al. 2007a).

In comparison to regional tsunami catalogues, radiocarbon dates obtained for cores PAL 7 and PAL 46 may suggest a possible relation to the earthquake of 551 AD which produced a tsunami that hit the Gulfs of Patras and Corinth (see Vött et al. 2006a for further references). The calibrated time bracket between 261–407 cal AD and 403–533 cal AD found for tsunami generation IV by dates for core PAL 6 in transect B (Table 1, Fig. 3), however, rather suggests a correlation with the 365 AD earthquake and tsunami catastrophe. This event is known by ancient accounts and geo-scientific studies to have strongly affected major parts of the eastern Mediterranean (Papazachos & Dimitriu 1991, Kelletat 1998, Sonnabend 1999, Stiros 2001, Stiros & Papageorgiou 2001, Scheffers 2006, Scheffers & Scheffers 2007, Shaw et al. 2008). We prefer this potential relation because of the more reliable sandwich dating strategy that could be applied in core PAL 6 and because the 365 AD event is reported to have reached as far as the Gulf of Venice (see Vött et al. 2006a). Generation IV tsunami deposits encountered in the Lake Voulkaria sediment trap would thus represent the first sedimentological and geochronological evidence of tsunami imprint on the coasts of the northwestern Ionian Sea by the 365 AD event.

Cleopatra's Canal seems to have been originally digged out of generation II and III event deposits (Fig. 3). This is also suggested by the elevation of the mentioned Roman bridge foundations (Section 2 and above, see also Vött et al. 2006a). We assume that the canal area was covered by thick layers of allochthonous material caused by event IV. In post-Roman times, both the canal and the spilled bridge remains were excavated again to re-establish the connection between the Lake Voulkaria and the Bay of Cheladivaron.

General discussion

At this point, we discuss the question if allochthonous sediments found in the environs of the Lake Voulkaria can be interpreted as sea level highstand deposits.

Initially, it has to be stated that there is no sedimentological and geomorphological evidence that the Lake Voulkaria represents the remains of a marine embayment formerly reaching across the Palairos coastal plain (Jahns 2005, Vött et al. 2006a, 2007b). Thus, marine deposits at the shores of the lake must have their origin in the littoral zone to the west of Aghios Nikolaos.

This study shows that marine sediments abruptly covering quiescent water deposits in the cores of central transect A at 7–3 m b.s.l. reflect high-energy dynamics. The Plaka beach ridge system as well as the Cheladivaron Promontory, a bedrock outcrop with elevations up to around 15 m a.s.l., serve as natural breakwaters for the inner Aghios Nikolaos Bay (Figs. 1 and 2). The Plaka structure has guaranteed predominantly lagoonal quiescent low-energy conditions in the Bay of Aghios Nikolaos, well protected from storms, at least since the 6th millennium BC (Vött et al. 2006a, 2007a, 2008b, 2008d). Theoretically, even a sea level highstand of several meters, no matter if of pre-Holocene or Holocene age, that would have exceeded the minimum elevation of 5 m a.s.l. of the Aghios Nikolaos bedrock sill would not have been able to induce high-energy littoral environments; this is true for the Bay of Cheladivaron and, all the more, for the sheltered Lake Voulkaria.

Additionally, previous studies on relative sea level evolution during the Holocene carried out along coastal Akarnania revealed that there has been a more or less continuous rise in sea level since the mid-Holocene (Vött 2007); intermediary highstands were not detected. Considering core ANI 1 where freshwater peat from a near-coast swamp was encountered at 8.31 m b.s.l. and radiocarbon dated to 5984–5895 cal BC (ANI 1/22 PR, Table 1), relative sea level in the outer Bay of Aghios Nikolaos was around or even below this depth in the 6th millennium BC. This corresponds well with relative sea level data from other Akarnanian sites (Vött 2007).

Sedimentological, palaeontological and micromorphological analyses revealed a multiple abrupt and partly chaotic input of allochthonous marine sediments into the lake. Faunal assemblages of different environments are mixed with angular mineral grains and organics from terrestrial origin (Figs. 5 and 6) which can only be explained by catastrophic inflow of sediment-loaded tsunami waves and not by sea level highstand. Comparable evidence of tsunami influence was found by Stanley & Bernasconi & (2006), Bernasconi et al. (2006) and Goiran (2001) for the ancient harbor of Alexandria, Egypt, and by Alvarez-Zarikian et al. (2008) for the Corinthian Gulf (see also Marriner & Morhange 2007). Moreover, sedimentary, macro- and microfaunal evidence of tsunami landfall in the inner Bay of Nikolaos was detected up to 6.70 m a.s.l. in the form of sandy to gravelly runup deposits, almost 20 cm thick (May et al. 2007) and rich in marine shell debris, and up to 14.80 m a.s.l. in the form of dislocated blocks and stones from the littoral zone covering the surface of the Cheladivaron Promontory (Vött et al. 2006a, 2008b). Considering the minimum elevation of the adjacent Aghios Nikolaos bedrock sill reaching around 5 m a.s.l. (Fig. 2, Section 2), this implicates strong tsunamigenic water inflow into the Lake Voulkaria. Multiple intersection of autochthonous lake deposits by allochthonous tsunamigenic sediments thus corresponds to findings of multiple tsunami impact detected for the entire Bay of Aghios Nikolaos and the adjacent coastal areas, namely the Sound of Lefkada and Actio Headland (Vött et al. 2006a, 2007a, 2008b, 2008c, 2008d, 2008e, May et al. 2007).

We assume that event deposits of younger generations encountered in cores ANI 24 to 27 and ANI 11 of transect A do not contain such fossil evidence because they were deposited above the relative sea level at the time of the event. Intense weathering led to decalcification, oxidation of organic material and soil formation. Thin section studies revealed that the clast-based skeleton of the sediments remained intact; it shows characteristics identically described for tsunami deposits still including marine shell debris (Fig. 5e and 5f, Section 4.2). Outstanding macro- and microfossil traces of tsunami impact are still preserved where deposition took place at or under sea level at the time of the event (Section 4, Fig. 3).

Independent of their age, the largest thickness of allochthonous deposits was found to the southeast of the Aghios Nikolaos bedrock sill. In terms of flow dynamics and transport energy, this corresponds to the hydraulic phenomenon that sudden divergence of rapid water currents after having overflowed a sill leads to immediate leeward and maximum accumulation of sediments due to the sudden decrease in energy (Section 6, Fig. 13). Also from this point of view, the stratigraphic constellations along transect A (Fig. 3) as well as the erosion channels detected by GPR measurements at the base of thick tsunami deposits (Fig. 8) cannot be explained by sea level highstand littoral dynamics. In fact, these findings show that inflowing tsunamigenic water currents were strongly channelized where the sill has its lowest elevation (Section 2, Fig. 2).

9 *Conclusions*

Within this study, sediment cores from the shores of the Lake Voulkaria (Akarnania, NW Greece) were investigated by sedimentological, micro- and macropalaeontological, micromorphological, computer tomographical and geochemical methods along two transects. Geophysical techniques allowed to detect subsurface structures and to interpolate between coring sites. The following conclusions can be made:

(i) Sediment cores from the Lake Voulkaria shores show that autochthonous quiescent water mud is repeatedly intersected by sandy to gravelly deposits which document temporary high-energy influence to the lake environment.

(ii) In many cases, intersecting coarse-grained layers reveal high amounts of shell debris of a fully marine macrofauna and ostracods and foraminifers mixed up with angular shaped mineral grains and organic material of mostly terrigenous origin. This indicates that high-energy influence came from the marine side and also affected terrestrial environments.

(iii) Layers of allochthonous material can be stratigraphically correlated along many kilometers along the Lake Voulkaria shores clearly decreasing in thickness with increasing distance from the Aghios Nikolaos bedrock sill.

(iv) The Plaka beachridge ruin as well as the Cheladivaron Promontory act as natural breakwaters and protect the inner Aghios Nikolaos Bay from storm influence. Intercalations of ex-situ material, however, reflect repeated high-energy impact on the lake from the Ionian Sea from a western direction. As they cannot be interpreted as sea level highstand deposits, these intercalations clearly represent tsunami events, thus corroborating geomorphological

and sedimentological traces of multiple tsunami landfall found by previous investigations for the outer Aghios Nikolaos Bay and its environs (Vött et al. 2006a, 2007a, 2008b, 2008c, May et al. 2007).

(v) Micromorphological studies of thin sections show that tsunamigenic material became subject to strong subaerial weathering including decalcification, oxidation and further soil formation processes where deposited above the sea level at the time of the event.

(vi) Geochronostratigraphic correlations between vibracores of transects A and B allowed to detect four different generations (I to IV) of tsunami impact on the inner Bay of Aghios Nikolaos and the Lake Voulkaria.

(vii) Relative age determination by palynological methods, radiocarbon dates and geoarchaeological findings helped to establish a local tsunami chronology. Generation I tsunami deposits encountered in the Bay of Cheladivaron probably are of mid-Holocene age (6th millennium BC). Tsunami II occurred around 1000 cal BC leaving traces on the western and southwestern shores and the profundal zone of the Lake Voulkaria. Generation III tsunami showed strongest impact on the western and only weak impact on the southwestern shores; its deposits may be attributed to an event during Classical-Hellenistic to maximum Roman times. Sedimentary traces of tsunami IV were found all along the lake shores and were time-bracketed to the 4th century AD. Our radiocarbon dates suggest a relation to the well known 365 AD catastrophe that devastated large parts of the eastern Mediterranean.

(viii) The comparison of tsunami traces from the Lefkada-Preveza coastal zone, known from previous studies, with tsunami imprint on the Lake Voulkaria reveals good accordance of both number and age of encountered tsunami deposits. However, thick layers of allochthonous marine sand and gravel encountered on the landward side of the Aghios Nikolaos bedrock sill require further dating efforts, especially by using OSL techniques.

In general, the naturally enclosed Lake Voulkaria allows an easy distinction between allochthonous and autochthonous sediments and, in some areas, revealed abundant organic material appropriate for radiocarbon sandwich dating of tsunami layers without adulterating marine reservoir effects. This makes the Lake Voulkaria to an outstanding and fairly reliable sediment trap for high-energy influence on the western coasts of continental Greece and the Ionian Islands.

Acknowledgements

Sincere thanks are due to K. Gaki-Papanastassiou, H. Maroukian and D. Papanastassiou (Athens) for joint field survey. We thank L. Kolonas (Athens), M. Stravropoulou (Mesolongion), C. Melisch (Berlin), U. Ewelt and R. Grapmayer (Grünberg), A. Schriever (Marburg), K. Ntageretzis (Köln) and S. Brockmüller (Landau) for support during field work and fruitful discussions. Radiocarbon analyses were accomplished by A. Scharf (Erlangen), P.M. Grootes (Kiel), and K. van der Borg (Utrecht). H.-J. Wagner and C. Georg (Marburg) carried out computer tomography analyses of core PAL 6. Work permits were issued by the Greek Institute of Geology and Mineral Exploration (Athens). We gratefully acknowledge funding of the research project by the German Research Foundation (Bonn, VO 938/2-1 and 3-1).

References

Alvarez-Zarikian, C.A., Soter, S. & Katsanopoulou, D. (2008): Recurrent submergence and uplift in the area of ancient Helike, Gulf of Corinth, Greece: Microfaunal and archaeological evidence. – J. Coastal Res. **24** (1a): 110–125.

Becker-Heidmann, P., Reicherter, K. & Silva, P.G. (2007): 14C-charcoal and sediment drilling cores as first evidence of Holocene tsunamis at the southern Spanish coast. – Radiocarbon **49** (2): 827–835.

Berkthold, P. & Faisst, G.W. (1993): Die Lage von Sollion. – Chiron **23:** 1–11.

Bernasconi, M.P., Melis, R. & Stanley, J.-D. (2006): Benthic biofacies to interpret Holocene environmental changes and human impact in Alexandria's Easter Harbour, Egypt. – The Holocene **16** (8): 1163–1176.

Beug, H.-J. (2004): Leitfaden der Pollenbestimmung für Mitteleuropa und angrenzende Gebiete. – Verlag Dr. Friedrich Pfeil, München, 542 pp.

Bousquet, B. & (1976): La Grèce occidentale. Interprétation géomorphologique de l'Epire, de l'Acarnanie et des îles Ioniennes. – Thèse l'Univ. Paris Sorbonne. Atelier reproduc. thèses de Lille III, Honore Champion, Paris, 585 pp.

Broadley, L., Platzman, E., Platt, J. & Matthews, S. (2004): Palaeomagnetism and tectonic evolution of the Ionian thrust belt, NW Greece. – In: Chatzipetros, A. & Pavlides, S. (eds.): Proceedings of the 5th International Symposium on Eastern Mediterranean Geology, 14–20 April 2004, Thessaloniki, Greece, Volume **II**, p. 973–976.

Bruins, H.J., MacGillivray, J.A., Synolakis, C.E., Benjamini, C., Keller, J., Kisch, H.J., Klügel, A. & van der Pflicht, J. (2008): Geoarchaeological tsunami deposits at Palaiokastro (Crete) and the Late Minoan IA eruption of Santorini. – J. Archaeol. Sci. **35:** 191–212.

Daux, G. (1960): Chronique des fouilles et découvertes archéologiques en Grèce en 1959. – Bull. Corresp. Héllenique **LXXXIV:** 617–871.

Dawson, A.G. (1994) Geomorphological effects of tsunami run-up and backwash. – Geomorph. **10** (1–4): 83–94.

Dawson, A.G. & Stewart, I. (2007): Tsunami deposits in the geological record. – Sediment. Geol. **200:** 166–183.

Dominey-Howes, D.T.M., Cundy, A. & Croudace, I. (2000): High energy marine flood deposits on Astypalaea Island, Greece: possible evidence for the AD 1956 southern Aegean tsunami. – Marine Geol. **163:** 303–315.

Dominey-Howes, D.T.M., Humphreys, G.S. & Hesse, P.P. (2006): Tsunami and palaeotsunami depositional signatures and their potential value in understanding the late-Holocene tsunami record. – The Holocene **16** (8): 1095–1107.

Earthquake Engineering Research Institute & (EERI, 2003): Preliminary observations on the August 14, 2003, Lefkada Island (Western Greece) earthquake. – EERI Spec. Earthquake Rep., 11 p., http://www.eeri.org/lfe/pdf/greece_lefkada_eeri_preliminary_ rpt.pdf [access: January 01, 2009].

Faisst, G.W. & Kolonas, L. (1990): Ein monumentaler Stufenaltar bei Palairos in Akarnanien. Vorläufiger Bericht. – Archäol. Anz. **1990:** 379–395.

Gaki-Papanastassiou, K., Maroukian, H., Papanastassiou, D., Palyvos, N. & Lemeille, F. (2001): Geomorphological study in the Lokrian coast of northern Evoikos Gulf (central Greece) and evidence of palaeoseismic destructions. – Rapp. et Proc.-verbaux Réun., Commiss. Int. l'Explor. Sci. Mer Méditerranée **36:** 25.

Geyh, M.A. (2005): Handbuch der physikalischen und chemischen Altersbestimmung. – Wiss. Buchgesell. Darmstadt, 224 pp.

Gianfreda, F., Mastronuzzi, G. & Sanso, P. (2001): Impact of historical tsunamis on a sandy coastal barrier: an example from the northern Gargano coast, southern Italy. – Nat. Hazards and Earth Sys. Sci. **1:** 213–219.

Goiran, J.-P. (2001): Recherches géomorphologiques dans la région littorale d'Alexandrie, Egypte. – PhD Thesis, Univ. Provence, Aix-en-Provence.

Hinsbergen, D.J.J. van, Langereis, C.G. & Meulenkamp, J.E. (2005): Revision of the timing, magnitude and distribution of Neogene rotations in the western Aegean region. – Tectonophysics **396:** 1–34.

Hollenstein, C., Müller, M.D., Geiger, A. & Kahle, H.-G. (2008): Crustal motion and deformation in Greece from a decade of GPS measurements, 1993–2003. – Tectonophysics **449:** 17–40.

Hughen, K.A., Baillie, M.G.L., Bard, E., Bayliss, A., Beck, J.W., Bertrand, C.J.H., Blackwell, P.G., Buck, C.E., Burr, G.S., Cutler, K.B., Damon, P.E., Edwards, R.L., Fairbanks, R.G., Friedrich, M., Guilderson, T.P., Kromer, B., McCormac, F.G., Manning, S.W., Bronk Ramsey, C., Reimer, P.J., Reimer, R.W., Remmele, S., Southon, J.R., Stuiver, M., Talamo, S., Taylor, Fw., van der Plicht, J. & Weyhenmeyer, C.E. (2004): Marine04 Marine radiocarbon age calibration, 26 – 0 ka BP. – Radiocarbon **46:** 1059–1086.

Institute of Geology and Mineral Exploration & (IGME) (1996): Geological map of Greece, 1:50,000. – Vonitsa Sheet, Athens.

Jahns, S. (2005): The Holocene history of vegetation and settlement at the coastal site of Lake Voulkaria in Acarnania, western Greece. – Veget. Hist. and Archaeobot. **14** (1): 55–66.

Jahns, S. (2007): Pollenanalytische Untersuchungen am Voulkaria-See zur Erforschung der Vegetations- und Umweltgeschichte der Plaghiá-Halbinsel. – In: Lang, F., Schwandner, E.-L., Funke, P., Kolonas, L., Jahns, S. & Vött, A. (eds.): Interdisziplinäre Landschaftsforschung im westgriechischen Akarnanien. – Archäol. Anz. **1/2007:** 179–190.

Jahns, S. (2009): The Holocene history of vegetation and environment of northern Akarnania, western Greece. – In: Mattern, T. & Vött, A. (eds.): Mensch und Umwelt im Spiegel der Zeit – Aspekte geoarchäologischer Forschungen in der antiken Welt. – Philippika, Marburger Altertumskundl. Abh. Vol. **1**. Harrassowitz, Wiesbaden, pp. 5–26.

Jankaew, K., Atwater, B.F., Sawai, Y., Choowong, M., Charoentitirat, T., Martin, M.E. & Prendergast, A. (2008): Medieval forewarning of the 2004 Indian Ocean tsunami in Thailand. – Nature **455:** 1228–1231.

Karakostas, V.G., Papadimitriou, E.E. & Papazachos, C.B. (2004): Properties of the 2003 Lefkada, Ionian Islands, Greece, earthquake seismic sequence and seismicity triggering. – Bull. Seismol. Soc. Amer. **94** (5): 1976–1981.

Kelletat, D. (1998): Geologische Belege katastrophaler Erdkrustenbewegungen 365 AD im Raum Kreta. – In: Olshausen, E. & Sonnabend, H. (eds.): Stuttgarter Kolloquium zur historischen Geographie des Altertums 6, 1996. – Naturkatastrophen in der antiken Welt. Stuttgart, pp. 156–161.

Kelletat, D. (2005): Neue Beobachtungen zu Paläo-Tsunami im Mittelmeergebiet: Mallorca und Bucht von Alanya, türkische Südküste. – In: Beck, N. (ed.): Neue Ergebnisse der Meeres- und Küstenforschung. – Schr. Arbeitskreis Landes- und Volkskunde Koblenz (ALV) **4:** 1–14.

Kelletat, D. & Schellmann, G. (2002): Tsunamis on Cyprus: Field evidences and ^{14}C dating results. – Z. Geomorph. N.F., Suppl. **137:** 19–34.

Kontopoulos, N. & Avramidis, P. (2003): A late Holocene record of environmental changes from the Aliki lagoon, Egion, North Peloponnesus, Greece. – Quatern. Int. **111:** 75–90.

Kortekaas, S. (2002): Tsunamis, storms and earthquakes: Distinguishing coastal flooding events. – PhD Thesis, Univ. .Coventry, Great Britain.

Kortekaas, S. & Dawson, A.G. (2007): Distinguishing tsunami and storm deposits: An example from Martinhal, SW Portugal. – Sediment. Geol. **200:** 208–221.

Lang, F., Schwandner, E.-L., Funke, P., Kolonas, L. & Freitag, K. (2007): Das Survey-Projekt auf der Plaghiá-Halbinsel 2000–2002. – In: Lang, F., Schwandner, E.-L., Funke, P., Kolonas, L., Jahns, S. & Vött, A. (eds.): Interdisziplinäre Landschaftsforschungen im westrgiechischen Akarnanien. Archäol. Anz. **1/2007**: 97–178.

Marriner, N. & Morhange, C. (2007): Geoscience of ancient Mediterranean harbours. – Earth-Sci. Rev. **80:** 137–194.

Mastronuzzi, G. & Sansò, P. (2000): Boulder transport by catastrophic waves along the Ionian coast of Apulia (southern Italy). – Marine Geol. **170** (1–2): 93–103.

Mastronuzzi, G. & Sansò, P. (2004): Large boulder accumulations by extreme waves along the Adriatic coast of southern Apulia (Italy). – Quatern. Int. **120:** 173–184.

Mastronuzzi, G., Pignatelli, C., Sansò, P. & Selleri, G. (2007): Boulder accumulations produced by the 20th of February, 1743, tsunami along the coast of southeastern Salento (Apulia region, Italy). – Marine Geol. **242:** 191–205.

May, S.M., Vött, A., Brückner, H. & Brockmüller, S. (2007): Evidence of tsunamigenic impact on Actio headland near Preveza, NW Greece. – In: Gönnert, G., Pflüger, B. & Bremer, J.-A. (eds.): Von der Geoarchäologie über die Küstendynamik zum Küstenzonenmanagement. – Coastline Rep. **9:** 115–125.

McCoy, F.W. & Heiken, G. (2000): Tsunami generated by the Late Bronze Age eruption of Thera (Santorini), Greece. – Pure Appl. Geophys. **157:** 1227–1256.

Minoura, K., Imamura, F., Kuran, U., Nakamura, T., Papadopoulos, G.A., Takahashi, T. & Yalciner, A.C. (2000): Discovery of Minoan tsunami deposits. – Geology **28** (1): 59–62.

Morhange, C., Marriner, N. & Pirazzoli, P.A. (2006): Evidence of late-Holocene tsunami events in Lebanon. – In: Scheffers, A. & Kelletat, D. (eds.): Tsunamis, hurricanes and neotectonics as driving mechanisms in coastal evolution. – Z. Geormorph. N.F. Suppl. **146:** 81–95.

Morton, R.A., Gelfenbaum, G. & Jaffe, B.E. (2007): Physical criteria for distinguishing sandy tsunami and storm deposits using modern examples. – Sediment. Geol. **200:** 184–207.

Murray, J.W. (2006): Ecology and applications of benthic foraminifers. – Cambridge Univ. Press, 426 pp.

Papadimitriou, P., Kaviris, G. & Makropoulos, K. (2006): The Mw = 6.3 2003 Lefkada earthquake (Greece) and induced stress transfer changes. – Tectonophys. **423:** 73–82.

Papadopoulos, G.A. Karastathis, V. K., Ganas, A., Pavlides, S., Fokaefs, A. & Orfanogiannaki, K. (2003): The Lefkada, Ionian Sea (Greece), shock (Mw 6.2) of 14 August 2003: Evidence for the characteristic earthquake from seismicity and ground failures. – Earth, Planets and Space **55** (11): 713–718.

Papazachos, B.C. & Dimitriu, P.P. (1991): Tsunamis in and near Greece and their relation to the earthquake focal mechanism. – In: Bernard, E.N. (ed.): Tsunami hazard. A practical guide for tsunami hazard reduction. – Nat. Hazards **4** (2–3): 161–170.

Papazachos, B.C. & Papazachou, C. (1997): The earthquakes of Greece. – Ziti, Thessaloniki, 304 pp.

Pareschi, M.T., Boschi, E. & Favalli, M. (2006): Lost tsunami. – Geophys. Res. Let. **33:** L22608.

Pirazzoli, P.A., Stiros, S.C., Arnold, M., Laborel, J. & Laborel-Geguen, F. (1999): Late Holocene coseismic vertical displacement and tsunami deposits near Kynos, Golf of Euboea, central Greece. – Phys. and Chem. Earth (A) **24** (4): 361–367.

Punt, W., Bos, J.A.A. & Hoen, P.P. (1991): Oleaceae (the Northwest European Pollen Flora 45). – Rev. Palaeobot. and Palynol. **69:** 23–47.

Reimer, P.J. & McCormac, F.G. (2002): Marine radiocarbon reservoir corrections for the Mediterranean and Aegean Seas. – Radiocarbon **44:** 159–166.

Reimer, P.J., Baillie, M.G.L., Bard, E., Bayliss, A., Beck, J.W., Bertrand, C.J.H., Blackwell, P.G., Buck, C.E., Burr, G.S., Cutler, K.B., Damon, P.E., Edwards, R.L., Fairbanks, R.G., Friedrich, M., Guilderson, T.P., Hogg, A.G., Hughen, K.A., Kromer, B., McCormac, F.G., Manning, S.W., Ramsey, C.B., Reimer, R.W., Remmele, S., Southon, J.R., Stuiver, M., Talamo, S., Taylor, F.W., van der Plicht, J., & Weyhenmeyer, C.E. (2004): IntCal04 Terrestrial radiocarbon age calibration, 26 - 0 ka BP. – Radiocarbon **46:** 1029–1058.

Reinhardt, E.G., Goodman, B.N., Boyce, J.I., Lopez, G., van Henstum, P., Rink, W.J., Mart, Y. & Raban, A. (2006): The tsunami of 13 December A.D. 115 and the destruction of Herod the Great's harbor at Caesarea Maritima, Israel. – Geology **34** (12): 1061–1064.

Sachpazi, M., Hirn, A., Clément, C., Haslinger, F., Laigle, M., Kissling, E., Charvis, P., Hello, Y., Lépine, J.-C., Sapin, M. & Ansorge, J. (2000): Western Hellenic subduction and Cephalonia Transform: local earthquakes and plate transport and strain. – Tectonophys. **319** (4): 301–319.

Scheffers, A. (2006): Coastal transformation during and after a sudden Neotectonic uplift in western Crete (Greece). – In: Scheffers, A. & Kelletat, D. (eds.): Tsunamis, hurricanes and neotectonics as driving mechanisms in coastal evolution. – Z. Geomorph. N.F. Suppl. **146:** 97–124.

Scheffers, A. & Scheffers, S. (2007): Tsunami deposits on the coastline of west Crete (Greece). – Earth and Planet. Sci. Let. **259** (3–4): 613–624.

Schielein, P., Zschau, J., Woith, H. & Schellmann, G. (2007): Tsunamigefährdung im Mittelmeer – Eine Analyse geomorphologischer und historischer Zeugnisse. – Bamberger Geograph. Schrift. **22:** 153–199.

Scicchitano, G., Monaco, C. & Tortorici, L. (2007): Large boulder deposits by tsunami waves along the Ionian coast of south-eastern Sicily (Italy). – Marine Geol. **238:** 75–91.

Shaw, B., Ambrayses, N.N., England, P.C., Floyd, M.A., Gorman, G.J., Highham, T.F.G., Jackson, J.A., Nocquet, J.-M. Pain, C.C. & Piggott, M.D. (2008): Eastern Mediterranean tectonics and tsunami hazard inferred from the AD 365 earthquake. – Nat. Geosci., http://www.nature.com/doifinder/10.1038/ngeo151.

Soloviev, S.L., Solovieva, O.N., Go, C.N., Kim, K.S. & Shchetnikov, N.A. (2000): Tsunamis in the Mediterranean Sea 2000 B.C. – 2000 A.D. – Kluwer, Dordrecht, 237 pp.

Sonnabend, H. (1999): Naturkatastrophen in der Antike. Wahrnehmung, Deutung, Management. – Metzler, Stuttgart, 270 pp.

Stanley, J.-D. & Bernasconi, M.P. (2006): Holocene depositional patterns and evolution in Alexandria's eastern harbor, Egypt. – J. Coast. Res. **22** (2): 283–297.

Stiros, S.C. (2001): The AD 365 Crete earthquake and possible seismic clustering during the fourth to sixth centuries AD in the Eastern Mediterranean: a review of historical and archaeological data. – J. Struct. Geol. **23** (2–3): 545–562.

Stiros, S. & Papageorgiou, S. (2001): Seismicity of western Crete and the destruction of the twon of Kisamos at AD 365: archaeological evidence. – J. Seismol. **5:** 381–397.

Vött, A. & (2007): Relative sea level changes and regional tectonic evolution of seven coastal areas in NW Greece since the mid-Holocene. – Quatern. Sci. Rev. **26:** 894–919.

Vött, A., Handl, M. & Brückner, H. (2002): Rekonstruktion holozäner Umweltbedingungen in Akarnanien (Nordwestgriechenland) mittels Diskriminanzanalyse von geochemischen Daten. – Geol. et Palaeontol. **36:** 123–147.

Vött, A., May, M., Brückner, H. & Brockmüller, S. (2006a): Sedimentary evidence of late Holocene tsunami events near Lefkada Island (NW Greece). – In: Scheffers, A. & Kelletat, D. (eds.): Tsunamis, hurricanes and neotectonics as driving mechanisms in coastal evolution. – Z. Geomorph. N.F. Suppl. **146:** 139–172.

Vött, A., Brückner, H., Schriever, A., Luther, J., Handl, M. & Borg, K. van der (2006b): Holocene palaeogeographies of the Palairos coastal plain (Akarnania, NW Greece) and their geoarchaeological implications. – Geoarchaeol. **21** (7): 649–664.

Vött, A., Brückner, H., May, M., Lang, F. & Brockmüller, S. (2007a): Late Holocene tsunami imprint on Actio headland at the entrance to the Ambrakian Gulf. – Méditerranée **108:** 43–57.

Vött, A., Brückner, H., Georg, C., Handl, M., Schriever, A. & Wagner, H.-J. (2007b): Geoarchäologische Untersuchungen zum holozänen Landschaftswandel der Küstenebene von Palairos (Nordwestgriechenland). – In: Lang, F., Schwandner, E.-L. Funke, P., Kolonas, L., Jahns, S. & Vött, A. (ed.): Interdisziplinäre Landschaftsforschung im westgriechischen Akarnanien. – Archäol. Anz. **1/2007:** 191–213.

Vött, A., May, S.M., Masberg, P., Klasen, N., Grapmayer, R., Brückner, H., Bareth, G., Sakellariou, D., Fountoulis, I. & Lang, F. (2008a): Tsunamite findings along the shores of the Eastern Ionian Sea – the Cefalonia case study (NW Greece). – In: Mastronuzzi, G., Sansò, P., Brückner, H. & Vött, A. (eds.): 2nd International Tsunami Field Symposium, Ostuni (Italy) and Ionian Islands (Greece), 22-27 September 2008. – GI^{2}S Coast Group Res. Publ. **6:** 167–170, Bari.

Vött, A., Brückner, H., May, M., Lang, F., Herd, R. & Brockmüller, S. (2008b): Strong tsunami impact on the Bay of Aghios Nikolaos and its environs (NW Greece) during Classical-Hellenistic times. – Quatern. Int. **181:** 105–122.

Vött, A., Brückner, H., Brockmüller, S., Handl, M., May, S.M., Gaki-Papanastassiou, K., Herd, R., Lang, F., Maroukian, H., Nelle, O. & Papanastassiou, D. (2008c): Traces of Holocene tsunamis across the Sound of Lefkada, NW Greece. – Global and Planetary Change, doi: 10.1016/j.glopacha.2008.03.015.

Vött, A., Brückner, H., Brockmüller, S., May, M., Fountoulis, I., Gaki-Papanastassiou, K., Herd, R., Lang, F., Maroukian, H., Papanastassiou, D. & Sakellariou, D. (2008d): Tsunami impacts on the Lefkada coastal zone during the past millennia and their palaeogeographical implications. – In: Papadatou-Giannopoulou, H. (ed.): Proceedings of the International Conference Honouring Wilhelm Dörpfeld, August 6-11, 2006. – Lefkada, Patras, pp. 419–438.

Vött, A., Brückner, H. & May, S.M. (2008e): Geomorphological, sedimentological and geoarchaeological traces of Holocene tsunami impact between Lefkada and the Lake Voulkaria and between Palairos and Preveza (NW Greece). – In: Mastronuzzi, G., Sansò, P., Brückner, H., Vött, A., Pignatelli, C., Caputo, R., Coppola, D., Di Bucci, D., Fracassi, U., May, S.M., Milella, M. & Selleri, G. (eds.): Palaeotsunami imprints along the coasts of the central Mediterranean Sea. – GI^2S Coast Group Res. Publ. **7:** 115–134, Bari.

Wacker, C. (1996): Die antike Stadt Palairos auf der Plagia-Halbinsel in Nordwest-Akarnanien. – In: Berkthold, P., Schmid, J. & Wacker, C. (eds.): Akarnanien. Eine Landschaft im antiken Griechenland. – Hrg. Oberhummer-Gesell. e.V. München. Ergon, Würzburg, pp. 91–98.

Addresses of the authors:
Prof. Dr. A. Vött (corresponding author: andreas.voett@uni-koeln.de), Dipl.-Geogr. S.M. May, Department of Geography, Universität zu Köln, Albertus-Magnus-Platz, 50923 Köln (Cologne), Germany.
Prof. Dr. H. Brückner, Dr. M. Handl, Faculty of Geography, Philipps-Universität Marburg, Deutschhausstr. 10, 35032 Marburg, Germany.
Dr. V. Kapsimalis, Dr. D. Sakellariou, Hellenic Centre for Marine Research, 19013 Anavissos, Greece.
Prof. Dr. O. Nelle, Ecology Centre, Department of Geobotany, Christian-Albrechts-Universität zu Kiel, Olshausenstr. 75, 24118 Kiel, Germany.
Prof. Dr. F. Lang, Department of Classical Archaeology, Technische Universität Darmstadt, El-Lissitzky-Str. 1, 64287 Darmstadt, Germany.
Dr. S. Jahns, Brandenburgisches Landesamt für Denkmalpflege und Archäologisches Landesmuseum, Wünsdorfer Platz 4-5, 15806 Zossen, Germany.
Prof. Dr. R. Herd, Faculty of Environmental Sciences and Process Engineering, Brandenburgische Technische Universität Cottbus, Karl-Marx-Str. 17, 03013 Cottbus, Germany.
Prof. Dr. I. Fountoulis, Department of Dynamic, Tectonic, Applied Geology, National and Kapodistrian University of Athens, Panepistimiopolis, 15784 Athens, Greece.